Transportation Infrastructure and City-Center Accessibility in the US and Europe[*]

Lucas Conwell[†]   Fabian Eckert[‡]   Ahmed Mushfiq Mobarak[§]

First Version: November 2022
This Version: July 2023

Abstract

We propose a theory-inspired measure of the accessibility to a city's central work location: the size of the surrounding area from which it can be reached within a specific time. Using publicly available optimal-routing software, we compute these "accessibility zones" for the 100 largest cities in the US and Europe, separately for cars and public transit commutes. Compared with European cities, US cities are half as accessible via public transit and twice as accessible via cars. Car accessibility zones are always larger than public transit zones, so that US cities are accessible from larger areas than European cities. However, population density within the most accessible zones is relatively low in the US, and European cities provide more residents quicker access to their city centers. Moreover, greater car orientation is associated with less green space, more congestion, and worse health and pollution externalities.

[†]Department of Economics, University College London; lucas.conwell@yale.edu
[‡]Department of Economics, University of California, San Diego; fpe@ucsd.edu
[§]Department of Economics and School of Management, Yale University; ahmed.mobarak@yale.edu

1. INTRODUCTION

The central business districts (CBDs) of the largest US cities account for an outsized fraction of the country's economic activity and growth. Therefore, broadening commuting access to these areas is an important policy objective. A wave of recent papers combines theory and data to evaluate existing or new transportation infrastructure in specific cities (Severen (2021) for Los Angeles, Tsivanidis (2022) for Bogotá, Allen and Arkolakis (2022b) for Chicago, and Kreindler et al. (2023) for Jakarta). However, no unified framework exists to quantify the accessibility of different cities via various modes of transport and to evaluate policy interventions.

In this paper, we propose a new measure of mode-specific commuting access to cities' central work locations that is (1) theory-consistent, (2) easy to compute for cities around the world, and (3) has an intuitive interpretation.

Our measure derives directly from the canonical urban model in economics, the Alonso-Muth-Mills framework (Brueckner, 1987). This framework highlights the tradeoff between commuting times and land prices that shapes the internal economic geography of cities. We demonstrate that as a direct corollary of this tradeoff, the welfare of the average city resident can be expressed as a weighted sum of the land areas around the central work location reachable within specific commuting times – which we refer to as "accessibility zones" – where the weights are decreasing in commuting time. More land within a short commute from the center allows for lower rents and shorter commutes for the average city resident, increasing welfare. As a result, the accessibility zones we introduce and construct in this paper are the welfare-relevant measure of city center accessibility.

Accessibility zones are easy to construct for most cities worldwide using standard travel-routing software. Using route-planning software from TravelTime Technologies, we compute the accessibility-zone areas of the 103 largest US and European cities. We compute the total land areas around cities' CBDs accessible within 0-15, 15-30, 30-45, and 45-60 minutes separately for public transit and car-based commutes during Wednesday morning rush hour. We use the resulting dataset to establish comparative facts about the accessibility of US and European cities' CBDs via car and public transit.

First, car accessibility zones are 2.8 times larger in US than in European cities

for commutes between 15 and 30 minutes, and this gap is even larger for commutes within 15 minutes. The average US city in our sample boasts 726 square kilometers from which the CBD can be reached within 15-30 minutes by car; the corresponding area is only 256 square kilometers in Europe.

Second, public transit accessibility zones are almost twice as large in European cities relative to comparably sized US cities for any specific time distance. The average size of the area from which CBDs of US cities can be reached within 15-30 minutes by public transit is 30 square kilometers, compared with 61 square kilometers in the average European city in our sample. However, US cities' public transit accessibility disadvantage appears less severe than informal public discourse suggests. This is because many US cities have bus-based public transit that uses the superior road infrastructure that serves cars.

Third, on average, car accessibility zones are almost an order of magnitude larger than public transit accessibility zones in both Europe and the US. As a result, US cities outperform Europe in terms of overall accessibility, given the relative strength of their car-based commuting systems.

Fourth, we show that population density within the most accessible zones (near city centers) is relatively low in the US compared to European cities. When we examine the *number of people with access* to CBDs (as opposed to the amount of land area), higher residential density in European cities amplifies their public transit advantage. European cities grant more than four times more workers transit access to its CBDs within 15 minutes compared to US cities. For car commutes, that higher residential density is sufficient to compensate for the land area advantage of US accessibility zones, and grant almost as many workers car access as in American cities.

The differences in residential density are likely to reflect, at least in part, a lack of residential housing development within US accessibility zones. US investments in car infrastructure create larger physical areas within a short commute from cities' CBD. However, investments in housing, urban design, or changes in land use policies are necessary to allow more Americans to relocate to those car-accessible areas. For the moment, in terms of people served, European cities enjoy a significant advantage, especially in the domain of public transit-based access to city centers, but even for car-based access.

Fifth, we show that the car-centric development in US cities not only fails to provide access to commuters, but also imposes larger indirect costs. Building

road and parking infrastructure to support car commutes creates stark tradeoffs regarding residential amenities and health. We borrow a clever insight from Baum-Snow (2007) – that the 1944 federal highway plan designed to support long-distance trade and national defense goals (as opposed to local commuting) creates some exogenous variation in highway infrastructure across US cities – to study the effects of car orientation on land use, pollution, and public health. Higher car orientation in cities – which we define as the ratio of car to public transit accessibility areas for a given time distance – is associated with much less green space within city boundaries, worse air pollution, less physical activity, worse health outcomes, and lower life expectancy.

Sixth, US cities' car-oriented urban design is associated with additional negative externalities. A comparison of the accessibility-zone areas during weekday rush hour and Sunday evening shows that heavy car usage slows car commutes due to congestion. Conversely, broad transit usage during rush hour *speeds up* transit commutes, which is likely related to the economies of scale in public transit provision.

The accessibility measure we develop can be a valuable empirical tool for researchers and policymakers to quantitatively analyze the tradeoffs inherent in urban design to inform future transportation policy choices. Our empirical work yields two important insights for urban policy.

First, car-based transportation systems are generally more effective at bringing workers from the city outskirts into the CBD. However, operating car-centric transportation systems comes at a cost to public health and the environment. Second, investments in road infrastructure to make physical space quickly accessible without complementary investments in housing infrastructure or changes to land-use policies fail to serve many city residents. The lack of residential density in US accessibility zones means that the potential of its superior road infrastructure to provide city-center access to large numbers of workers has been left unrealized in practice.

Related Literature. A closely related literature in urban planning has studied various notions of urban access beginning with Hansen (1959) and Ingram (1971). The most widely used measure of "access" in this literature is the average commuting time between workers' residences and their job locations in a city (Wu and Levinson, 2020; Bento et al., 2005). These measures combine (a) the location choices of firms and workers, (b) the travel-mode choices of workers, and (c) the efficacy of different modes in the transportation system. In

contrast, our measure of infrastructure-enabled CBD accessibility conceptually separates the efficiency of the commuting system from the location *choices* of firms and workers.

A broad class of recent quantitative spatial models of commuting combines commuting flows, wage and rent data, and structural parameters into a "sufficient statistic measure of realized equilibrium commuting access" (e.g., Monte et al., 2018; Tsivanidis, 2022). We show that accessibility zone areas are the welfare-relevant measure of commuting access in a large sub-class of these quantitative spatial models; accessibility zones have the advantage that they can be easily computed for cities around the world and used to evaluate the effectiveness of transportation policies in real time.

An emerging literature in urban economics employs navigation and route-finding software tools to study urban mobility. In pioneering work, Akbar et al. (2021) and Couture et al. (2018) use the Google Maps route-finding feature to measure car travel speeds at different times of the day in the US and India. Kreindler (2022) measures traffic density using GPS records of trips collected via a smartphone app. Miyauchi et al. (2021) use smartphone GPS data for Japan to establish new facts about city travel patterns. Our approach is related but different: we use an algorithm from TravelTime Technologies that calculates optimal routes between arbitrary points via different modes and aggregates these points into areas that fall below a certain travel-time threshold.

The paper has the following structure. In Section 2, we show that our accessibility measure emerges as the natural welfare-relevant measure of commuting access in the canonical model of within-city commuting in urban economics. Section 3 describes the construction of accessibility-zone areas in the data and presents descriptive statistics of driving versus public transit in the US versus Europe. Section 4 discusses the relationship between accessibility-zone areas and land use, health, and environmental outcomes.

2. Theory

In classic models of within-city location choices of workers the central trade-off is that between commuting times and rents (see, e.g., Brueckner (1987), Ahlfeldt et al. (2015), Monte et al. (2018), and Redding and Rossi-Hansberg (2017)). In equilibrium low rents compensate for long commuting times and vice versa.

We present a quantitative version of the classic models and show that its central trade off implies that the welfare of the average resident depends on the amount of residential land available at different distances from the central work location. We derive all theoretical results in this section in Appendix A.

2.1 A Model of Commuting

Setup. We consider a closed city economy inhabited by a mass $\bar{L} = 1$ of agents who work in a central business district (CBD).[1] We subdivide the city into $i = 1, ..., N$ residential locations of equal geographic area $A_i = A = 1$. Locations differ in their mode-specific commuting times to the CBD. Each agent has Cobb-Douglas preferences over residential land, with share α, and the final good.[2] Agents choose a residential location as well as their consumption of land and the final good to maximize their utility.

Labor Demand. In the CBD, a representative firm produces a homogeneous final good using a labor-only constant returns to scale technology. Input and output markets are competitive, and trade is free. Thus, workers receive their fixed marginal product, denoted by w, and the final good's price is constant across locations and serves as a convenient numeraire. Following the tradition of within-city urban models, the CBD wage is hence parameter of the model (see Brueckner (1987)).

Labor Supply. Commuting between location i and the CBD via mode m incurs a utility cost $(1 - \tau_i^m) \in (0, 1)$.[3] To facilitate aggregation, we assume that agents draw idiosyncratic preference shifters $\eta_i^m(\omega)$ for each location independently from identical Fréchet distributions, $F(\eta) = \exp\{-\eta^{-\theta}\}$, where $\theta > 0$ indexes the heterogeneity of tastes for a given location-mode combination among agents. Workers spend a fixed share α of their income on residential land and the rest on the consumption of the final good. Therefore, the utility of a worker ω who lives in location i and commutes using mode m is given by $V_i^m(\omega) = w(1 - \tau_i^m)r_i^{-\alpha}\eta_i^m(\omega)$, where r_i denotes the rental rate per unit of land in location i.

---

[1] We provide a more general treatment with multiple work destinations in the Appendix.

[2] The assumption that workers have preferences over residential land instead of housing services is innocuous. In Appendix A.3, we present an extension of our model in which a competitive housing sector produces housing services using fixed land and the final good.

[3] In this formulation, commuting time takes away from time spent enjoying leisure. Instead of modeling leisure explicitly, we assume commuting lowers utility directly.

Aggregation and Equilibrium. Under our standard Fréchet assumption, utility maximization by individuals implies that the fraction ϕ_i^m of agents that live in location i and commute into the CBD via mode m is given by:

$$(1) \qquad \phi_i^m = \frac{\left(1 - \tau_i^m\right)^\theta w^\theta r_i^{-\alpha\theta}}{\sum_{k,m} \left(1 - \tau_k^m\right)^\theta w^\theta r_k^{-\alpha\theta}}.$$

Within each location, the rental rate adjusts to clear the land market:

$$(2) \qquad r_i A_i = \alpha w \sum_m \phi_i^m.$$

The model's equilibrium system comprises Equations 1 and 2; together, they pin down equilibrium rental rates and population-mode shares in each location, i.e., $\{r_i\}_i$ and $\{\phi_i^m\}_{i,m}$.

Equilibrium Welfare. The model also provides an expression for the welfare, u, of the average worker:

$$(3) \qquad u = \Gamma\left(1 - \frac{1}{\theta}\right)\left[w^\theta \sum_{i,m}(1 - \tau_i^m)^\theta r_i^{-\theta\alpha}\right]^{1/\theta}$$

Equation 3 shows that higher commuting times or rents in any location decrease welfare while a higher wage increases welfare.[4]

We can use Equations 1 and 2, as shown in Appendix A.1, to express a monotone transformation $\bar{u}$ of welfare in terms of parameters:

$$(4) \qquad \bar{u} := \sum_{i,m}(\psi_i^m)^{\frac{\theta - \iota}{\theta}}(1 - \tau_i^m)^\iota A_i^{\frac{\theta - \iota}{\theta}} \quad \text{where} \quad \psi_i^m = \frac{(1 - \tau_i^m)^\theta}{\sum_m(1 - \tau_i^m)^\theta}.$$

Note that ψ_i^m is the fraction of residents in location i that commute to work using mode m.[5] The composite parameter $\iota := \theta(1 - \frac{\theta\alpha}{1 + \theta\alpha}) \in (0, \theta)$ measures the importance of commuting costs and land availability relative to idiosyncratic motives in individuals' residential location choices. Equation 4 shows that welfare in the city depends on the amount of land available at different commuting distances from the center; land at shorter commuting distances provides greater

---

[4]The expression in Equation 3 also corresponds to the ex-ante expected welfare of each worker before learning their preference shocks.

[5]In Appendix A.1, we present a generalization of the formula in Equation 4 for cities with many work locations. The formula in Equation 4 is a particular case of our more general formula.

welfare benefits. For given mode shares, the area accessible at different commuting distances is thus the welfare-relevant measure of a city's commuting accessibility.

In Appendix A.1, we present a generalization of Equation 4 for cities with many work locations which generates the same central insights. Furthermore, in Appendix A.3, we present an extension of our model in which a competitive housing sector produces housing services using fixed land and the final good. Only the magnitudes of the exponents in Equation 4 change; their signs and all other conclusions remain unaffected.[6]

2.2 Towards an Empirical Measure of CBD Accessibility

To move towards an empirically tractable measure of commuting accessibility, we assume that locations offer one of several discrete commuting times, indexed by κ, and that commuting times increase in κ, $\partial \tau / \partial \kappa > 0$. Denote the set of locations i that share the same commuting time κ via mode m by $\Lambda^m(\kappa)$. We can then rewrite Equation 4 as

$$(5) \qquad \bar{u} = \sum_m \sum_\kappa (1 - \tau(\kappa))^\iota \bar{\psi}^m(\kappa) \mathcal{A}^m(\kappa)$$

where $\mathcal{A}^m(\kappa)$ is the total land area accessible via mode m in κ minutes and $\bar{\psi}^m(\kappa)$ is a measure of the fraction of mode m commuters among all residents in $\mathcal{A}^m(\kappa)$.[7] Figure 1 shows accessibility zones of an example city for two different modes of transports, car ($m = C$) and public transit ($m = P$) and for different commuting times $\kappa = 1, 2, 3, 4$. The figure makes clear that different land parcels can belong to different accessibility zones for different modes. The figure also shows that accessibility zones do not necessarily have to be contiguous.

Equation 5 demonstrates that city welfare increases with the number of land parcels available within short commutes of the CBD via each mode, weighted by (inverse) commute times and mode shares. Importantly, these weights reflect both the direct dis-utility from long commutes and the fact that fewer workers will endogenously choose to live in areas with long commutes, despite

---

[6]In Appendix A.4, we also show that a version of our formula holds in the classic monocentric city model without idiosyncratic preferences.

[7]In particular, we have that $\bar{\psi}^m(\kappa) = \frac{1}{|\Lambda^m(\kappa)|} \sum_{i \in \Lambda^m(\kappa)} (\psi_i^m)^{\frac{\theta - \iota}{\theta}}$.

cheaper residential land. For example, cities with poor public transportation systems would have small corresponding accessibility zones for every level of commute time κ and thus lower welfare. Areas accessible by public transit at only on high-κ commutes receive a low weight $(1 - \tau(\kappa))^\iota$, so enlarging them would not appreciably raise welfare. Thus, successful commute systems require *both* large areas and short commute times, and the *accessibility zone* areas $\mathcal{A}^m(\kappa)$ serve as sufficient statistics for the welfare benefits of a city's commute system, conditional on worker mode choices.

FIGURE 1: EXAMPLE ACCESSIBILITY ZONES FOR DIFFERENT MODES
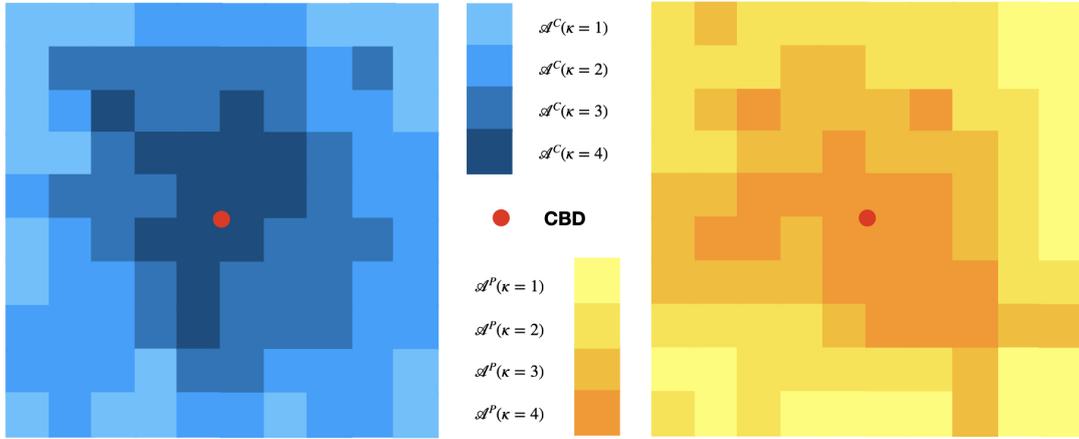
Notes: This figure shows example accessibility zone for a city consisting of 100 parcels of land for two different modes (cars, $m = C$, and public transit, $m = P$) and four different commuting times. The red dot indicates the location of the central business district in which all work takes places. Darker shades indicate accessibility zones associated with lower costs of commuting.

Our paper, therefore, focuses on measuring $\mathcal{A}^m(\kappa)$ for a large sample of cities to generate policy-relevant insights. The size of accessibility zones for a given city depends not only on the quality of the physical infrastructure (e.g., streets and rail lines) but also on the utilization of these routes (e.g., through congestion) and the frequency of and connectivity between different transit options. In the next section, we describe how we overcome these measurement challenges and then present facts which speak to critical transportation policy questions. Have some US cities been more successful than others at creating large accessibility zones for their workers? How do accessibility zones compare across different modes of transport? Are US cities systematically worse at creating large accessibility zones than cities elsewhere? What can we learn from the cross-section of US cities about the societal implications of enlarging the accessibility zones

for cars versus for public transit?

2.3 Housing Supply versus Land Supply

Policy frictions such as zoning and land-use restrictions may break the correspondence between raw land area and the actual housing supply available to workers. Suppose workers instead have preferences over exogenously-supplied housing. Our welfare measure then additionally depends on the housing supply $\mathcal{H}^m(\kappa)$ available at different commuting distances κ from the CBD via the density of residential development $h^m(\kappa) := \mathcal{H}^m(\kappa)/\mathcal{A}^m(\kappa)$ in the accessibility zone:

$$(6) \qquad \bar{u} = \sum_m \sum_\kappa (1 - \tau(\kappa))^\iota \bar{\psi}^m(\kappa) h^m(\kappa) \mathcal{A}^m(\kappa).$$

The area of the accessibility zone and the density of its development correspond to two different policy instruments, namely transportation infrastructure and land-use regulations, to enhance access to the CBD. In other words, area yields the *potential* space available to accommodate commuters while density reflects a city's fulfillment of that potential. Given our primary focus on transportation infrastructure, we first present measures of accessibility zone areas in the next section and later introduce proxies for the density of development within them.

3. ACCESSIBILITY-ZONE AREAS IN THE DATA

The vast majority of commutes in the 103 European and American cities in our sample occur via either public transit or car and take less than 60 minutes.[8] Accordingly, we focus our measurement on car ($m = C$) or public transit ($m = P$) commutes that take less than 60 minutes. We split the 60 minutes into four 15-minute intervals, and denote the resulting accessibility zones by $\mathcal{A}^m_{t,t+\Delta}$ for $t = 0, 15, 30, 45$ and $\Delta = 15$.

---

[8]Tables D.7 and D.8 in the Appendix provide the complete list of cities. Across all the US cities in our sample, 96% of commuters into the CBD use car or public transit; of those, only 12% have commutes above 60 minutes.

3.1 Constructing Accessibility Zones

We aim to study commutes into the primary CBD. Statistical agencies generally do not provide a ready-to-use definition of the location of a city's CBD. We follow existing papers and define the center of the CBD as the latitude and longitude coordinates generated by feeding the city's name into Google's Geocoding Application Programming Interface (API) (see Holian and Kahn, 2012; Couture and Handbury, 2020; Couture et al., 2021).[9] We refer to the area that falls within a one-kilometer radius around these coordinates as the CBD. The median US CBD in our sample accounts for 28% of all employment within a 20 kilometer radius around the CBD. Seventy-seven percent of CBDs defined in this way include one of the top-three highest average income ZIP codes in the respective city. We study the robustness of our accessibility zone measures to the single CBD assumption below.

The ubiquity of modern travel-routing software makes computing accessibility zones feasible for most major cities worldwide. Software such as Google Maps allows users to quickly find the fastest mode-specific route from any origin to any point within the CBD at a specific time of day. For public transit, such software uses the actual schedules of all buses, trains, subways, and trams in making travel time predictions. For cars, it takes into account predicted traffic congestion.

We first describe how one would use Google Maps to construct accessibility zones, given most readers' familiarity with the tool. First, divide the city into parcels of land. The smaller the parcels, the more accurate the borders of each zone. Use Google Maps to compute the travel time between the centroid of each parcel and the closest point in the CBD, separately for car and public transit commutes. Then group parcels into accessibility zones within 0-15, 15-30, 30-45, or 45-60 minutes' commute time to the CBD, separately for the two modes. Summing the area of all parcels within each time interval (e.g., 0-15) yields the total accessibility-zone area, $\mathcal{A}^m_{t,t+\Delta}$.[10]

---

[9]Holian and Kahn (2012) report that "although this method of identifying CBDs places considerable trust in Google's potentially ad-hoc definitions of central places, we found them to be quite reasonable in all cases."

[10]Each parcel belongs to only one (mutually exclusive) accessibility zone for a given mode. However, a parcel could be in the 30-minute zone for car commutes and the 15-minute zone for public transit commutes. Accessibility zones are not necessarily contiguous. For example, workers who live near subway stations can often reach the CBD faster than from other areas closer to the CBD in terms of their straight-line distance.

FIGURE 2: ACCESSIBILITY ZONE AREAS

(A) PUBLIC TRANSIT

(B) DRIVING

Minutes of Travel | 0-15 | 15-30 | 30-45 | 45-60
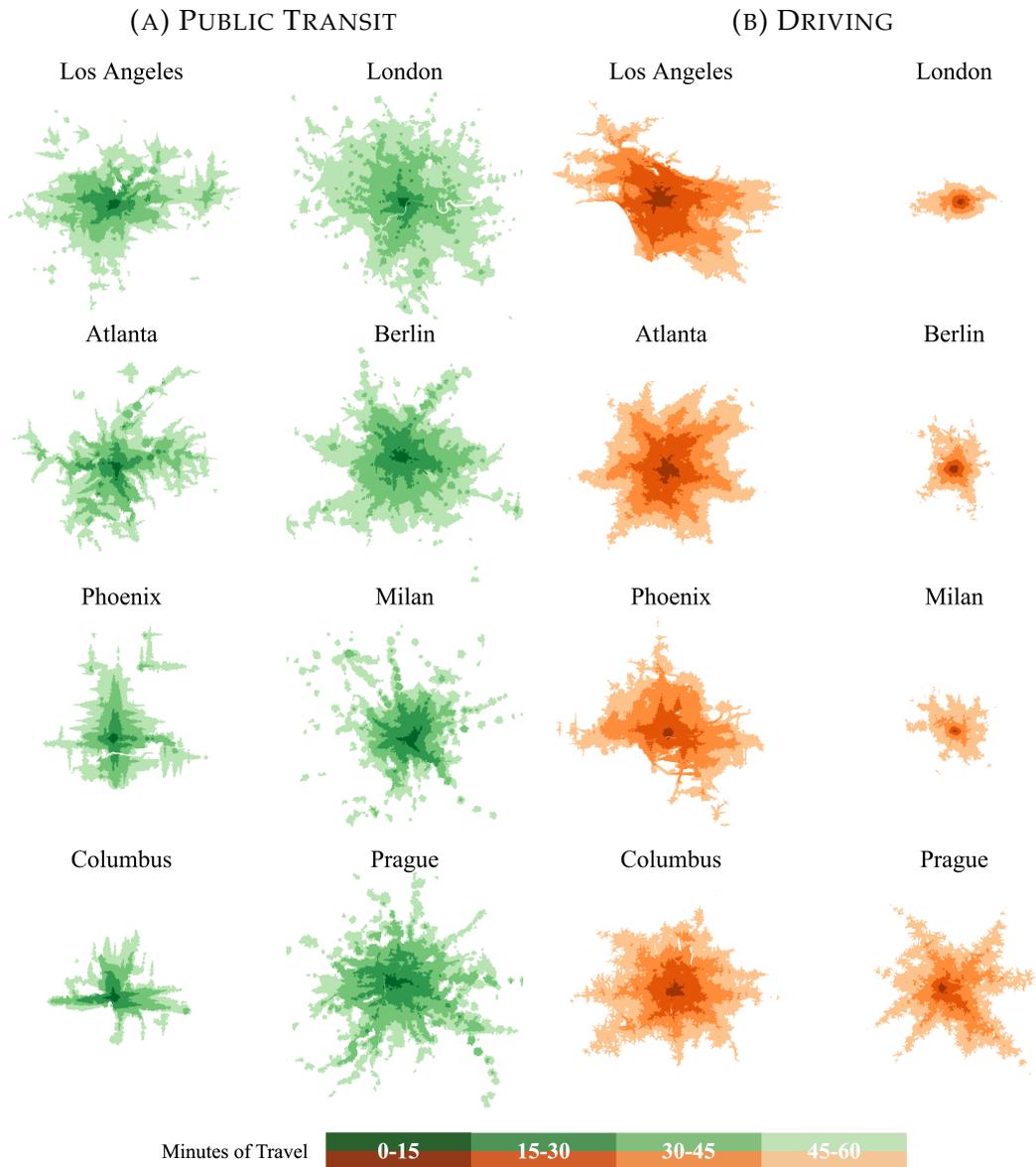
Notes: The figure shows the area reachable from a city's CBD within 0-15, 15-30, 30-45, and 45-60 minutes ("accessibility zones") for four US and four European cities, with comparable-population metro areas placed next to each other. The left panel shows the accessibility zones for public transit commutes (green), and the right panel shows the accessibility zones for car-based commutes (orange) that arrive in the CBD at 8:45 AM on a Wednesday. The (0,15)-minute accessibility-zone area has the darkest, and the (45,60)-minute accessibility-zone area has the lightest hue. All accessibility zones for a given mode appear on the same scale; the size of the public transit zones in Panel (A) is inflated by a factor of 3, relative to the driving zones in Panel (B), for readability.

In practice, we use TravelTime Technologies's Isochrone API, which automates

the process described above.[11] TravelTime's calculations use publicly-available schedule API data for public transit in all major cities and account for waiting times, walking time to and from transit, and time spent traversing stations. For driving, the algorithm uses "OpenStreetMap," an open-source API that provides data on the complete road infrastructure and street-specific speed profiles for most countries. The corresponding calculations account for traffic congestion patterns, traffic lights, and the time required to park the car at the destination.

We use the Traveltime API to obtain the area from which the CBD of a given city can be reached within 15, 30, 45, and 60 minutes on a Wednesday at 8:45 AM, separately for public transit users and drivers. We then subtract the (0,15)-minute area from the (0,30)-minute area to obtain the (15,30) accessibility-zone area and so on, yielding the $\mathcal{A}_{t,t+\Delta}^m$ for all cities in our sample.

We explore the robustness of the resulting accessibility zones to alternative construction procedures. First, we re-do our exercise using a different software provider, Targomo, which provides the same service.[12] Second, instead of relying on proprietary software, we construct accessibility zones using the Google Maps API and Python.[13] Table B.1 in the Appendix shows the high correlations between the areas of accessibility zones constructed using the different approaches.

3.2 Comparing Accessibility across Modes and Countries

Figure 2 shows accessibility zones $\{\mathcal{A}_{t,t+\Delta}^m\}_{t=0,15,30,45}^{m=C,T}$ for a sample of cities. Public transit zones are shown in green in the two columns on the left, and car zones in orange on the right. Darker hues indicate shorter travel times, and each row features comparable-population US and European cities side-by-side. Note that car accessibility zone areas are substantially larger than the public transit areas. To show them side-by-side in the same figure, we reduced the relative scale of

---

[11]See https://app.traveltime.com/ for the web app to use this data product. The app works for any country for which online mapping services are available.

[12]https://www.targomo.com/

[13]We use the GoogleMaps API to obtain mode-specific travel times between any two points and perform a grid search over a given number of rays radiating outward from the destination. We start at some given distance and then move inward or outward along each ray until reaching the given time threshold, say, 60 minutes. The envelope of the final 60-minute points along each ray delineates one of our accessibility zones. This approach misses spatial discontinuities in access that are important for public transit and well-captured by TravelTime's algorithm.

12

the driving accessibility zone areas by a factor of three.

Figure 2 highlights some important patterns generalize to the full sample of cities. First, US cities' car accessibility zones are generally larger than those of European cities with comparable population sizes. Second, the opposite is true for public transit zones. Third, the fact that we had to reduce the scale of the car zones to fit them into the figure highlights that the infrastructure supporting car travel in US cities affords the greatest overall accessibility.

Insights from the Full Sample. Table 1 displays the average accessibility-zone areas in square kilometers, separately by mode, region, and time distance and confirms that the insights from Figure 2 generalize to the full sample of cities. The "Car" panel on the left shows that, depending on the time interval, car accessibility zones are 1.3-4 times larger in the US than in Europe. The US car advantage is most pronounced for short commutes between 0 and 15 minutes, perhaps reflecting the difficulty of navigating the dense cores of old European cities by car. The "Public Transit" panel in the middle shows that transit zones in US cities are only approximately half the size of those of European cities, regardless of the commuting distance.

Table 1 also shows that car travel offers larger overall accessibility across all time intervals in both Europe and the US; that is $\mathcal{A}^C_{t,t+15} > \mathcal{A}^P_{t,t+15} \forall t \in \{0, 15, 30, 45\}$. Figure 2 highlights one reason why public transit systems provide less access to CBDs than cars. Especially at longer distances from the CBD, public transit provides "patchy" access. Only people who live very close to the sparse network of transit stops in outlying parts of cities can quickly access the CBD. By contrast, car-based access is spatially more continuous. Because they have a comparative advantage in car-based commutes, US cities thus enjoy greater accessibility overall.

Variation Across Cities. The two panels in the top row of Figure 3 show the relationship between accessibility and city size. We graph the areas of the (0,60)-minute car accessibility zones, $\mathcal{A}^C_{0,60}$, and the (0,60)-minute public transit accessibility zones, $\mathcal{A}^P_{0,60}$, against city size, separately for the US and Europe. In the US, the size of car accessibility zones does not vary with city population. By contrast, car accessibility zones are smaller in larger European cities, perhaps because their older urban cores are dense, congestion-prone, and difficult for cars to navigate.

Public transit accessibility zone areas are increasing in city size on both conti-

13

Min.	Car			Public Transit			Car/Public Transit		
	US	Europe	Ratio	US	Europe	Ratio	US	Europe	Ratio
0-15	85.94	21.72	3.96	3.86	6.65	0.58	26.84	4.45	6.03*
15-30	725.95	256.05	2.84**	29.70	61.17	0.49***	31.04	5.65	5.49**
30-45	1493.27	863.23	1.73***	91.18	160.05	0.57***	18.85	6.41	2.94**
45-60	2260.38	1702.59	1.33***	149.93	262.01	0.57***	19.22	7.65	2.51**

Notes: This figure shows average accessibility-zone areas for various time intervals and modes in the US and Europe. The third column in the "Car" and "Public Transit" panels shows the ratio of the preceding two numbers in the respective row. The "Car/Public Transit" panel shows averages, across cities, of the ratio of the car relative to public transit accessibility-zone areas ("car orientation") for each time interval and region. The last panel's third column shows the ratio of US cities' car orientation relative to European cities' car orientation. We conducted Wald tests in all columns with a "Ratio" header for the null hypothesis that the ratio equals 1. The number of stars indicates the p-value with the following interpretation: *** $p<0.01$, ** $p<0.05$, * $p<0.1$.

nents, reflecting the economies of scale inherent in mass public transit, which has high fixed setup costs and low marginal costs for cities. A more extensive ridership base permits investments in larger transit systems, higher station density, and train frequency.

The other four panels show the distribution of $\{\mathcal{A}_{0,15}^{C}, \mathcal{A}_{0,15}^{P}, \mathcal{A}_{45,60}^{C}, \mathcal{A}_{45,60}^{P}\}$ across our samples of US and European cities. US and European cities are most dissimilar when focusing on (0,15)-minute accessibility zones. Most European cities have very small $\mathcal{A}_{0,15}^{C}$, and there is little heterogeneity. US cities differ widely in their (0,15) car accessibility-zone areas, and almost all US cities have larger zones than European cities. Conversely, most European cities outperform every US city in terms of (0,15)-minute public transit accessibility. Several European cities have substantially larger zones than even New York City, the single US outlier in the $\mathcal{A}_{0,15}^{P}$ panel.

European and US cities are more similar in terms of their (45,60)-minute accessibility zones, but the US's comparative advantage remains in cars, and Europe's in public transit. These patterns of comparative advantage are the result of offsetting factors that only come into play at greater distances from the CBD. The "patchiness" of public rail transit access in particular makes covering large areas far away from the CBD difficult, so European rail-based transit becomes less efficient on the outskirts of cities. At the same time, bus-based transit in the US leverages existing road infrastructure and thus helps render long-distance transit more comparable to that of European cities. Conversely, the relative

disadvantage of cars in the dense urban cores of European cities diminishes in more suburban areas.

FIGURE 3: ACCESSIBILITY ZONES ACROSS CITIES

(A) $\mathcal{A}^C_{0,60}$

(B) $\mathcal{A}^P_{0,60}$

(C) $\mathcal{A}^C_{0,15}$

(D) $\mathcal{A}^P_{0,15}$

(E) $\mathcal{A}^C_{45,60}$

(F) $\mathcal{A}^P_{45,60}$
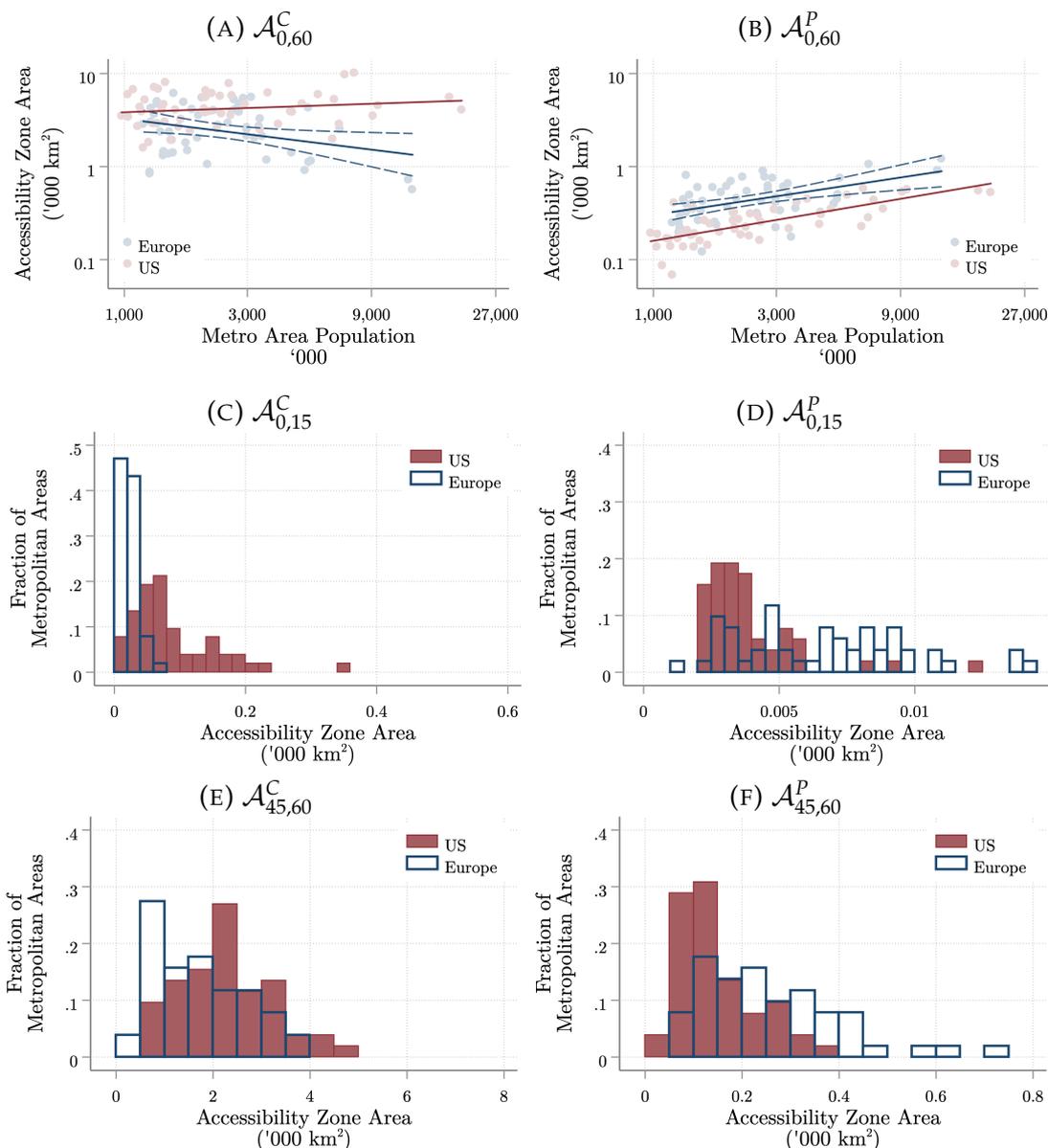
Notes: Panel (A) shows a scatter plot of an OECD metro area's population size against its (0,60)-minute accessibility-zone area for cars, separately for the US (red) and Europe (blue); it also shows linear best-fit lines and 95% confidence intervals for the Europe fit line. Panel (B) replicates Panel (A) but instead shows (0,60)-minute public transit accessibility-zone areas. Panels (C)-(D) show histograms of the (0,15)-minute accessibility-zone areas for all cities in our sample for cars (left) and public transit (right), separately for the US and Europe. Panel (E)-(F) replicates Panels (C)-(D) for the (45,60)-minute accessibility-zone areas. All accessibility-zone areas in the figure are for commutes that arrive in the CBD at 8:45 AM on a Wednesday.

15

3.3 Robustness Checks

Polycentric versus Monocentric Cities. We have computed accessibility zones around a city's *single* CBD as identified by Google Maps. We now conduct a robustness test to check whether relaxing this single-CBD assumption fundamentally changes our insights. We gather data on total payroll and employment by ZIP code from the Census County Business Patterns files for 2015 to identify the ZIP codes within each city with the highest total payroll per square meter. We define a city's employment centers as the ZIP codes with the highest payroll density that jointly account for 10% of the corresponding metro area's total payroll. Using this procedure, we identify several geographically distinct employment centers for many American cities in our sample. For example, in New York City, clusters of adjoining ZIP codes near Midtown East, Madison Square Garden, and Wall Street emerge as distinct employment centers.[14]

For every US city in our sample, we compute accessibility zones around each employment center and then take the outer envelope of these accessibility zones to define *polycentric* accessibility zone areas from which at least one of a city's employment centers can be reached within t minutes.

Table D.1 displays the results of this exercise. At short distances, allowing for multiple CBDs roughly doubles accessibility zone areas, but for longer distances, accessibility zone areas remain fairly similar to our baseline *monocentric* case. This convergence reflects the fact that most employment clusters which this new procedure uncovers lie close to each other, near city centers. However, the relative sizes of car and transit accessibility zones remain similar. Even the *poly*centric public transit zones in US cities are smaller than their (relatively more conservative) *mono*centric European transit counterparts.

Park and Ride. Some public transit systems feature so-called "Park and Ride" infrastructure where users drive to large parking lots at rail transit stations and then ride the subway or commuter rail to the city center. Ignoring this possibility may stack the deck in favor of cars. Our software allows us to compute accessibility zones for park-and-ride commuting for cities in the US and UK. We compute accessibility zones for such a park-and-ride hybrid mode, where we allow commuters to drive up to 15 minutes to a rail transit stop and then

---

[14]We lack the required data to construct multiple employment centers for all European cities in a similar fashion.

TABLE 2: DRIVING VERSUS PUBLIC TRANSIT ACCESSIBILITY-ZONE AREAS

Correlation	US		Europe		Pooled	
	Value	Std. Error	Value	Std. Error	Value	Std. Error
$(\mathcal{A}^C_{0,15}, \mathcal{A}^P_{0,15})$	-0.347	0.248	-0.308	0.196	-0.326**	0.155
$(\mathcal{A}^C_{15,30}, \mathcal{A}^P_{15,30})$	-0.214	0.162	-0.0642	0.220	-0.107	0.140
$(\mathcal{A}^C_{30,45}, \mathcal{A}^P_{30,45})$	0.327**	0.148	0.361*	0.196	0.350***	0.125
$(\mathcal{A}^C_{45,60}, \mathcal{A}^P_{45,60})$	0.392*	0.206	0.630***	0.115	0.570***	0.0992

Notes: The table reports the coefficients from a regression of the log of the $(t, t+\Delta)$-minute driving accessibility-zone area on the log of the $(t, t+\Delta)$-minute public transit accessibility-zone area, run separately for $t = 0, 15, 30, 45$, $\Delta = 15$, and various samples. The "US" panel reports these coefficient estimates for a regression run with 52 US cities; the "Europe" panel reports the same coefficients for regressions run in our European sample of 51 cities. The "Pooled" panel reports coefficients from running the regression in the pooled Europe and US samples controlling for a Europe fixed effect. All regressions control for log OECD metro area population and include a constant. Robust standard errors in parentheses: *** p<0.01, ** p<0.05, * p<0.1.

transfer to a train for the rest of the journey.

The park-and-ride option does enlarge transit accessibility zones for a few cities, as shown in Figure D.1. However, for most cities, the sizes of transit zones change little; transit systems in most American cities rely on buses which lack park-and-ride options. Appendix Table D.2 highlights the 18 US and UK cities in our sample for which the hybrid park-and-ride 45-60 minute accessibility zone is larger than the corresponding zone for public transit alone. In summary, the insights about American and European commuting systems we highlight by comparing driving to pure public transit are not deeply affected by the possibility of hybrid-mode commuting.

3.4 Are Driving and Transit Infrastructure Substitutes?

Do the evident US specialization in cars and European specialization in public transit imply car- and transit-based development strategies are substitutes? Table 2 shows how the sizes of the driving and transit accessibility-zone areas co-vary in the cross-section of cities, within regions and in the pooled sample. The table presents conditional correlations between accessibility-zone areas for cars and transit, controlling for city population and a Europe fixed effect in the pooled specification.

The substitutability or complementarity of transit and driving accessibility varies

17

with distance from the CBD. The conditional correlation between $\mathcal{A}_{0,15}^C$ and $\mathcal{A}_{0,15}^P$ suggests a trade-off between transit and car orientation at short time distances close to city centers. On average, cities with larger (0,15)-minute car accessibility zones have smaller public transit zones. In and around the city centers, transit and car infrastructure act as substitutes. Farther out from the CBD, the sizes of car and transit accessibility zones correlate positively. This complementarity may stem from the prevalence of bus transit, especially in US cities. Better road infrastructure for cars also aids bus-based mobility.

Accessibility, Infrastructure, and Mode Choices. Appendix C explores how accessibility-zone areas correlate with direct measures of road and public transit infrastructure as well as commuter mode choices.

The miles of rail lines in a city is significantly positively correlated with $\mathcal{A}_{0,60}^P$ in both Europe and the US, but not with $\mathcal{A}_{0,60}^C$, as expected (Table C.1). Conversely, the length of the road network is more positively correlated with $\mathcal{A}_{0,60}^C$ than $\mathcal{A}_{0,60}^P$. Accessibility-zone areas will therefore likely respond to commuting infrastructure investments.

Table C.2 shows that commuter mode choices are correlated with the size of the accessibility-zone area for the corresponding mode in the cross-section of cities. Car accessibility-zone areas are associated with increases in the share of commuters who drive and decreases in the share taking transit to work. Transit accessibility zones $\mathcal{A}_{0,60}^P$ are associated with a reduction in the share of commuters driving and increases in both public transit use and walking/biking. Thus, future changes in accessibility zones will likely translate into sizable commuter mode shifts. The presence of such a relationship highlights the appropriate use (and limits) of our measures for policy analysis.

3.5 Housing Supply versus Land Supply

We have thus far focused on computing accessibility zones' land areas, but Equation 6 in Section 2.3 underscores that housing supply within these zones determines how many commuters can take advantage of that accessibility in reality. Since we cannot directly measure housing supply at a sufficiently high spatial resolution for our full sample of cities, we employ the total number of people living within each accessibility zone as a proxy. Such data are available for all cities in our sample from the European Commission's Global Human Settlement Layer Project.

Table 3 reproduces Table 1 for population density within each accessibility zone instead of area in order to proxy for the density of residential development $\frac{\mathcal{H}^m(\kappa)}{\mathcal{A}^m(\kappa)}$. The accessibility zones associated with lower commuting times to the CBD appear more efficiently used in Europe than in the US. The substantially smaller European car accessibility zones are nonetheless 2-3 times more densely populated than their American counterparts at every time interval. The same is true for the European public transit accessibility-zone areas which, recall, also surpass the US zones in raw area.

These findings suggest that much of the US advantage in road-served land area (Table 1) will disappear when we consider the total *number of people* served by that infrastructure. Table 4, where we compute the total residential population within each accessibility zone, confirms this intuition. Even though European car accessibility zones are substantially smaller, the total number of people living within a given number of minutes of the CBD by car is comparable in the US and Europe. Superior US car infrastructure quickly connects larger land areas to the CBD, but evidently, land use policies in the US waste this potential. US policymakers could improve overall accessibility if, via housing and land-use policies, they could induce more people to live in the zones where existing road infrastructure provides quick access to the CBD. On the public transit side, European accessibility zones are larger and more densely populated, amplifying the European advantage in Table 4's middle panel. European cities provide CBD access to more than four times as many workers within 0-30 minutes as US cities.

Currently, the US falls short on most counts: it has smaller public transit accessibility zones than Europe and, even within these zones, has failed to achieve European levels of residential density. Moreover, its extensive car infrastructure provides access to vast areas of only thinly populated land.

4. THE EXTERNALITY COST OF AMERICAN CITIES' CAR ORIENTATION

Any discussion of whether to prioritize car or public transit infrastructure investments to increase CBD accessibility must also consider that these approaches are likely associated with very different amenities and environmental and public health externalities. The transportation policy literature has highlighted sev-

TABLE 3: AVERAGE ACCESSIBILITY-ZONE POPULATION DENSITY BY REGION AND MODE

Min.	Car			Public Transit			Car/Public Transit		
	US	Europe	Ratio	US	Europe	Ratio	US	Europe	Ratio
0-15	2845.71	10156.64	0.28***	3953.04	11601.79	0.34***	0.82	0.87	0.94
15-30	1594.23	5054.32	0.32***	3303.13	7975.15	0.41***	0.51	0.58	0.87*
30-45	740.52	1998.94	0.37***	2537.88	4258.53	0.60***	0.30	0.41	0.73***
45-60	359.23	809.45	0.44	1999.14	2362.16	0.85	0.18	0.32	0.56***

Notes: This figure shows average accessibility-zone population density (total population/area) for various time intervals and modes in the US and Europe. The third column in the "Car" and "Public Transit" panels shows the ratio of the preceding two numbers in the respective row. The "Car/Public Transit" panel shows averages, across cities, of the ratio of the car relative to public transit accessibility-zone population density for each time interval and region. The last panel's third column shows the ratio of US cities' mean relative car accessibility zone density to European cities' mean relative car accessibility zone density. We conducted Wald tests in all columns with a "Ratio" header for the null hypothesis that the ratio equals 1. The number of stars indicates the p-value with the following interpretation: *** p<0.01, ** p<0.05, * p<0.1.

TABLE 4: AVERAGE ACCESSIBILITY-ZONE POPULATIONS (TOTAL IN THOUSANDS) BY REGION AND MODE

Min.	Car			Public Transit			Car/Public Transit		
	US	Europe	Ratio	US	Europe	Ratio	US	Europe	Ratio
0-15	191	167	1.14	18	85	0.22	23.74	3.95	6.01**
15-30	1036	801	1.29	119	501	0.24***	15.36	2.57	5.98
30-45	1036	1053	0.98	269	660	0.41***	5.14	1.85	2.77
45-60	696	1036	0.67***	359	627	0.57***	2.61	1.88	1.39

Notes: This figure shows average accessibility-zone total raw populations (in thousands) for various time intervals and modes in the US and Europe. The third column in the "Car" and "Public Transit" panels shows the ratio of the preceding two numbers in the respective row. The "Car/Public Transit" panel shows averages, across cities, of the ratio of the car relative to public transit accessibility-zone populations ("population car orientation") for each time interval and region. The last panel's third column shows the ratio of US cities' population car orientation to European cities' population car orientation. We conducted Wald tests in all columns with a "Ratio" header for the null hypothesis that the ratio equals 1. The number of stars indicates the p-value with the following interpretation: *** p<0.01, ** p<0.05, * p<0.1.

eral different categories of externalities commonly associated with commuting systems (see Appendix Figure D.2 from Khreis et al., 2017) including congestion, land use, health, and pollution. We use these categories to organize our discussion of the externalities associated with car versus public transit accessibility.

4.1 Congestion Externalities

Our theoretical framework did not explicitly model the dependence of commuting costs on the number of commuters using a given mode-route combination. In reality, commute times are often a function of the intensity of use, so the size of accessibility zones may depend on the time of the day. We use our accessibility measure to construct a straightforward test for the direction of such usage externalities. We re-compute our (0,60)-minute accessibility zones for each mode ($\mathcal{A}^m_{0,60}$) for commutes to the CBD that arrive on a Sunday at 11 PM ("Off-Peak Hours"). At that time, traffic on routes into the CBD should be much lower than on a Wednesday at 8:45 AM ("Peak Hours"), the timing, recall, we have used thus far in the paper. The change in $\mathcal{A}^m_{0,60}$ between peak and off-peak hours gives us a sense of the direction and size of congestion effects on each mode.

The left panel of Figure 4 graphs peak-hour car accessibility-zone areas against off-peak areas. Each point represents a city in our sample. All points fall below the 45-degree line, which implies that the size of the area reachable from the CBD within 60 minutes expands during off-peak hours–a negative congestion externality. About 35% of the land area that falls within 60 minutes of the CBD during off-peak hours is no longer accessible within 60 minutes during rush hour in the median city.

The right panel of Figure 4 conducts the same exercise for public transit accessibility zones, with opposite results: median public transit accessibility is 56% *larger* during peak than off-peak hours. These findings likely reflect the economies of scale in (shared) public transit provision: running buses and trains more frequently becomes profitable when more people use the system simultaneously.

The opposite signs of the car and transit usage externalities complicate any policy recommendations for improving a city's commuting access. Building more roads could slow car commutes via induced demand (Duranton and Turner,

FIGURE 4: HOW ACCESSIBILITY-ZONE AREAS CHANGE WITH USAGE

(A) Driving, $\mathcal{A}_{0,60}^{C}$

(B) Public Transit, $\mathcal{A}_{0,60}^{P}$
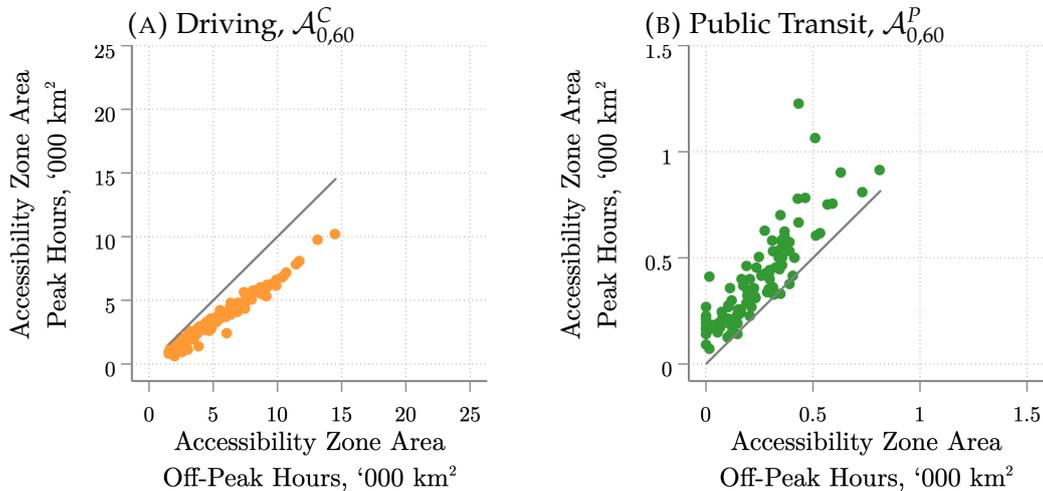
Notes: This figure shows scatter plots of cities' accessibility-zone areas during peak (Wednesday 8:45 AM) and off-peak (Sunday 11 PM) hours. The left panel is for car-based commutes, and the right is for public-transit-based commutes. Both panels also include a 45-degree line for reference.

2011). On the other hand, building better public transit could, via general-equilibrium forces, lead to higher train frequency and station density. This improved overall performance of the transit system would then generate additional commuting-access gains.

4.2 Correlations with Land Use, Health, and Pollution

Next, we report a set of conditional correlations by regressing land use, health, and pollution outcomes on $\mathcal{A}_{0,60}^{C}$ and $\mathcal{A}_{0,60}^{P}$, controlling for other observable determinants of those outcomes as suggested by the relevant literature. We restrict our analysis to the US cities in our sample, due to a lack of consistent data for European cities.

Methodology. Because the land use, health, and pollution outcomes are available at the county level, we employ a two-step procedure to make the most use of the available county-level variation and maximize the statistical power of our analysis. In the first step, we run county-level regressions of each outcome (e.g., road density or PM2.5 pollution) on a set of control variables, such as a county's average socioeconomic or geographic characteristics and its manufacturing orientation. We aggregate the residuals of this first-step regression up to the city level and, in a second step, regress those residuals on our city-level

TABLE 5: THE COSTS OF ACCESSIBILITY

Panel A: Land Use

	Log Total km per km^2			Green-space	Walking
	Motorway	Streets	Bike Lanes	per km^2	Index
$\log \mathcal{A}^P_{0,60}$	0.0489	0.0252	0.216	-0.0432	0.810
	(0.143)	(0.0957)	(0.769)	(0.0440)	(0.523)
$\log \mathcal{A}^C_{0,60}$	0.490***	0.207**	0.347	-0.127***	-0.902***
	(0.0996)	(0.101)	(0.443)	(0.0430)	(0.310)
R^2	0.234	0.140	0.187	0.271	0.133

Panel B: Direct Health Externalities

	Share Physically Inactive	Sh. Poor + Far from Groceries	Share Obese	Deaths per 1000	
				Traffic	Obesity
$\log \mathcal{A}^P_{0,60}$	-0.0221**	-0.00309	-0.00593	-0.401*	-0.0499
	(0.00858)	(0.00825)	(0.00777)	(0.202)	(0.269)
$\log \mathcal{A}^C_{0,60}$	0.0136*	0.0287***	0.0290***	0.166	0.532***
	(0.00744)	(0.00760)	(0.00637)	(0.155)	(0.188)
R^2	0.148	0.254	0.321	0.073	0.164

Panel C: Pollution Externalities

	t/yr			log Mean	Aug. Temp
	$\log CO_2$	$\log NOx$	$\log PM2.5$	Noise	p90/p10
$\log \mathcal{A}^P_{0,60}$	0.0441	-0.00113	0.0112	0.000671	-0.0248
	(0.106)	(0.164)	(0.183)	(0.00507)	(0.0345)
$\log \mathcal{A}^C_{0,60}$	0.357***	0.398***	0.310**	0.00224	-0.0398
	(0.0687)	(0.112)	(0.138)	(0.00327)	(0.0245)
R^2	0.285	0.213	0.093	0.014	0.029

Panel D: Indirect Health Externalities

	Deaths per 1000			Premature	log Life
	Asthma	COPD	Total	Deaths/100k	Expectancy
$\log \mathcal{A}^P_{0,60}$	0.0292	-0.158	10.59*	0.0823	-0.00974
	(0.0682)	(0.787)	(5.531)	(0.0557)	(0.00637)
$\log \mathcal{A}^C_{0,60}$	0.115*	2.266***	6.109	0.0956**	-0.0131***
	(0.0637)	(0.651)	(4.042)	(0.0392)	(0.00444)
R^2	0.163	0.226	0.224	0.290	0.350

Notes: All regressions control for the corresponding OECD metro area population in the second stage. Robust standard errors in parentheses. *** p<0.01, ** p<0.05, * p<0.1. We add 1e-6 to the bike lanes to avoid zeros. All regressions are run on our sample of the 52 largest US cities, save for the motorway and street length specifications which omit Los Angeles. We present a complete list of data sources in Appendix Table D.5; Appendix Table D.6 presents summary statistics including the mean and median of every outcome variable.

measures of $\mathcal{A}_{0,60}^C$ and $\mathcal{A}_{0,60}^P$, along with a control for metro area population. Our two-step procedure allows us to report correlations that condition on the more-disaggregated county-level determinants of each outcome variable.

Land Use. Car- and public transit-based access require different types of physical infrastructure which likely translate into urban land-use decisions. We explore this possibility in the top panel of Table 5.[15] The second-step associations between (the unexplained variation in) land-use outcomes and $\mathcal{A}_{0,60}^C$ as well as $\mathcal{A}_{0,60}^P$ indicate that cities with larger car accessibility zones have significantly more space allocated to streets and motorways per square kilometer of city land. Given car accessibility, public transit accessibility and road density do not exhibit a significant association. The correlation of the size of transit accessibility zones with bike-lane density is positive, but not statistically significant.

Next, we see that the road density which improves car accessibility takes land away from other uses. A 10% increase in the car accessibility-zone area ($\mathcal{A}_{0,60}^C$) is associated with a 1.3-percentage-point decrease in the share of green space. Green space only accounts for about 9% of the total land area surrounding the average US CBD in our sample, making this effect sizable. A 10% increase in the car accessibility-zone area is also associated with an 0.09-point decrease in the city's 20-point "walkability index."[16] By contrast, a 10% increase in public transit accessibility area is associated with an 0.08-point *improvement* in the city's walkability index, but this estimate is not statistically significant.

Health. Panel B of Table 5 examines health outcomes commonly associated with car usage.[17] A 10% increase in $\mathcal{A}_{0,60}^C$ is associated with a 0.14-percentage-point increase in the share of the population that is physically inactive. By contrast, a 10% increase in the public transit accessibility zone area $\mathcal{A}_{0,60}^P$ has the opposite association: a 0.2-percentage-point *decrease* in the physically inactive share. Likewise, a 10% increase in car accessibility is associated with a 0.29-percentage-point increase in the share of the population in the city that is both

---

[15]Controls in the first stage of our land-use regressions include the fraction of owner-occupied housing, log population density, log income per capita, the share of black and Hispanic residents, mean democratic vote share, log mean temperature in January, and the agricultural+mining share of employment.

[16]The EPA's National Walkability Index is a composite score of Census block groups' relative amenability to pedestrian trips on a 1-20 scale and accounts for street-intersection density, proximity to transit stops, and land-use diversity.

[17]First-stage controls include the shares of black residents, Hispanic residents, residents above age 65, residents with heavy drinking habits, smokers, and log population density.

poor and lacks easy access to groceries.[18] In other words, car accessibility is a positive predictor of "food deserts" (Allcott et al., 2019). Car accessibility is also associated with a larger share of the population that is obese.

Next, we use administrative cause-of-death data from the US Center for Disease Control and find a positive but insignificant correlation between traffic deaths and $\mathcal{A}_{0,60}^C$ as well as a marginally-significant negative correlation between traffic deaths and $\mathcal{A}_{0,60}^P$. Obesity deaths, however, are statistically larger when cities are designed for car accessibility.

Pollution. Panel C shows that car accessibility displays a strong positive association with air pollutants commonly associated with the burning of fossil fuels, including CO_2, NOx, and $PM2.5$, with elasticities of 0.31-0.4; transit accessibility does not.[19] No correlation exists between car accessibility and noise pollution emitted by transportation sources or a measure of urban heat islands.

Mortality. Our regressions provide suggestive evidence that more acute pollution, physical inactivity, obesity, and food deserts translate into downstream health outcomes such as mortality and life expectancy. More car-accessible cities have a higher rate of deaths from asthma and chronic pulmonary diseases (COPD) as well as a higher premature death rate, holding constant the county-level demographic variables that predict these outcomes. A 10% increase in $\mathcal{A}_{0,60}^C$ is associated with a 0.13% decrease in life expectancy among residents. Transit accessibility-zone areas do not significantly correlate with any mortality outcome.

In summary, car accessibility is associated with negative externalities in pollution, health, and land use within our sample of US cities. These relationships are generally consistent with prior literature in economics that has studied the effects of transportation on land use (Glaeser and Kahn, 2010; Duranton and Puga, 2015), pollution (Parry et al., 2007; Gendron-Carrier et al., 2022; Schlenker and Walker, 2016), and health (Knittel et al., 2016; Currie and Walker, 2011). Our findings also echo Adler and van Ommeren (2016)'s study of trade-offs between modes as well as a public health literature which links urban transport policy and mode choices, the built environment, and health outcomes (Khreis et al., 2017).

---

[18]"Poor" are residents with incomes below twice the poverty line. "Lack of easy access" refers to living more than one mile from the nearest grocery store.

[19]First-stage controls include log income per capita, log population density, the urban share of the population, the share of employment in manufacturing (CBP), and log county centroid latitude.

4.3 Instrumenting for Car Orientation

Section 4.2 is careful to use the language of "correlation" to describe the connections between $\mathcal{A}_{0,60}^C$, $\mathcal{A}_{0,60}^P$ and land use, pollution, or health to avoid interpreting associations as causal relationships. $\mathcal{A}_{0,60}^C$ and $\mathcal{A}_{0,60}^P$ may be correlated with other unmeasured characteristics of cities that independently affect pollution or mortality.

To explore causal connections, we borrow an insight from Baum-Snow (2007): we study the effects of *car orientation* ($\mathcal{A}_{0,60}^C / \mathcal{A}_{0,60}^P$) on land use, pollution, and health by instrumenting ($\mathcal{A}_{0,60}^C / \mathcal{A}_{0,60}^P$) with the 1947 interstate highway plan drawn up by the National Interregional Highway Committee, designed to "connect...the principal metropolitan areas, cities, and industrial centers, to serve the national defense." The basis for this plan, the 1944 Federal Aid Highway Act, never mentions local commuting as a design goal. While the actual highway network constructed after 1956 in consultation with state and local governments was indeed responsive to local commuting demand, using the 1947 plan as an instrument allows us to extract the portion of the road infrastructure that cities received because of their fortunate positioning vis-a-vis the federal government's ambitions to facilitate national defense and long-distance trade. Baum-Snow (2007) shows that while actual urban highway construction responds to local commuting demand and is likely endogenous, the 1947 plan did not.

In Table 6, we take the ratio of $\mathcal{A}_{0,60}^C$ to $\mathcal{A}_{0,60}^P$ to construct a single RHS variable we call "car orientation" because we only have a single instrument. This ratio increases when larger tracts of land are quickly accessible from the CBD by car but not by public transit. The first stage of the IV regression shows that the 1947 highway plan is indeed predictive of subsequent car dependence: cities that received an additional highway ray passing through their CBDs in the 1947 National Highway plan did experience an increase in their actual car orientation, measured in 2021 through our procedure of computing $\mathcal{A}_{0,60}^C$ and $\mathcal{A}_{0,60}^P$, by 0.102, or 0.2 standard deviations. Following Baum-Snow (2007), we hold constant the metro area population by including it as a control variable because the 1947 plan may have allocated more highways to bigger cities. While our instrument predicts car orientation in the expected direction, the first-stage F-stat of 5.7 raises concerns about a weak instrument. We, therefore, report Anderson-Rubin confidence intervals robust to weak instruments (Andrews et al., 2019)

throughout in Table 6. The corresponding OLS results are reported in Appendix Table D.4.

The instrumented results are broadly consistent with the correlations we observed in Section 4.2, but we lose some statistical precision. Greater car orientation today stemming from the 1947 federal highway plans statistically significantly increases contemporaneous air pollution. The effect sizes also appear quantitatively meaningful: a standard deviation increase in car orientation increases NOx by almost a full standard deviation. It also affects land use, decreasing green space in the city by a full standard deviation. There are also statistically significant adverse effects on health, with a one standard deviation increase in car orientation lowering life expectancy by 0.02 years.

5. CONCLUSION

Our research highlights a fundamental trade-off in the design of commuter systems. Cars are generally more effective at providing city-center access to far larger surrounding land areas – and therefore potential populations – than public transit in both the US and Europe. However, the superior accessibility car-based transit creates is only realized if the density of housing development keeps pace. We show that European cities, because they manage to create much higher residential density in their accessibility zones, end up providing greater access to city centers via both cars and public transit than US cities.

In addition, car-based commuting imposes larger negative externalities and health costs on society. Cities designed for greater car accessibility to CBDs suffer from higher pollution and less-walkable neighborhoods. Their residents are more physically inactive and obese; as a result, car-oriented cities have greater mortality rates and lower life expectancy in the cross-section. By contrast, transit accessibility is not associated with such adverse effects.

The current car orientation of the US is a result of post-World War II policy choices to invest heavily in roads and highways. Part of that highway infrastructure – designed to last 50-70 years – is now approaching its expiration date (New York Times, Feb. 11, 2022), and cities must weigh the costs and benefits of alternative policy directions.[20] Many cities, such as Syracuse and Detroit,

---

[20]The Biden administration's infrastructure plan reflects some potential changes in the focus of transportation policy; see (Los Angeles Times, November 11, 2021).

	Panel A: Land Use				
	Log Total km per km^2			Green-space	Walking
	Motorway	Streets	Bike Lanes	per km^2	Index
$\log\left(\mathcal{A}_{0,60}^C / \mathcal{A}_{0,60}^P\right)$	1.372**	0.593*	0.931	-0.384*	-0.676
	(0.632)	(0.354)	(1.681)	(0.219)	(0.815)
Weak IV-Robust CI	[.50, 6.36]	[.02, 3.00]	[-3.10, 9.84]	[-2.13, -.03]	[-2.76, 3.45]
	Panel B: Direct Health Externalities				
	Share	Sh. Poor		Deaths per 1000	
	Physically	+ Far from	Share		
	Inactive	Groceries	Obese	Traffic	Obesity
$\log\left(\mathcal{A}_{0,60}^C / \mathcal{A}_{0,60}^P\right)$	0.0175	0.0923*	0.0468*	-0.920	0.861
	(0.0141)	(0.0484)	(0.0257)	(0.681)	(0.551)
Weak IV-Robust CI	[-.04, .07]	[.02, .50]	[-.01, .19]	[-7.69,-.04]	[-.16, 4.65]
	Panel C: Pollution Externalities				
		t/yr		log Mean	Aug. Temp
	$\log CO_2$	$\log NOx$	$\log PM2.5$	Noise	p90/p10
$\log\left(\mathcal{A}_{0,60}^C / \mathcal{A}_{0,60}^P\right)$	1.348**	1.628**	1.478**	0.0122	-0.334
	(0.553)	(0.709)	(0.695)	(0.0107)	(0.228)
Weak IV-Robust CI	[.67, 6.98]	[.71, 8.67]	[.58, 8.44]	[-.01, .08]	[-2.22, .02]
	Panel D: Indirect Health Externalities				
	Deaths per 1000			Premature	log Life
	Asthma	COPD	Total	Deaths/100k	Expectancy
$\log\left(\mathcal{A}_{0,60}^C / \mathcal{A}_{0,60}^P\right)$	0.142	3.797**	18.27	0.386**	-0.0364**
	(0.205)	(1.916)	(12.46)	(0.191)	(0.0183)
Weak IV-Robust CI	[-.41, 1.13]	[.11, 16.37]	[-8.65, 92.18]	[.11, 2.03]	[-.17,-.004]
	Panel E: First Stage				
Planned Rays in 1947		.102** (.043)		*Effective 1st-Stage F:* 5.700	

Notes: All regressions instrument for log relative car to public transit accessibility zone area with the number of interstate highway rays passing through the corresponding metropolitan area's central city CBD according to the original 1947 plan from Baum-Snow (2007) and control for OECD metro area population. Robust standard errors in parentheses. *** p<0.01, ** p<0.05, * p<0.1. We additionally report the effective first-stage F statistic following Olea and Pflueger (2013) as well as 95% Anderson-Rubin confidence sets robust to weak instruments (Andrews et al., 2019). All regressions use 51 of our 52 largest US cities, due to missing data on the instrument for Las Vegas; the motorway and street length specifications also omit Los Angeles.

have committed to replacing stretches of interstate with more connected, walkable neighborhoods.[21] Other cities, such as Houston, are expanding their highway systems in an attempt to make CBDs more accessible (Los Angeles Times, November 11, 2021).

These forthcoming transportation infrastructure investments will affect how US residents live, work, and commute over the next 50 years. As a result, city planners should consider not only the productivity and efficiency effects of focusing on roads versus public transit infrastructure but also the social, environmental, congestion, and health consequences of their choices. The CBD accessibility measures we propose, by virtue of their replicability across cities, times of day, and repeatedly over time, can aid such policy evaluations.

Study Limitations and Directions for Future Work. Our study is descriptive by design: we construct a theory-consistent, easy-to-implement measure of CBD accessibility to aid policy analysis.

Transportation infrastructure or large-scale densification programs necessarily have general equilibrium effects on within-city traffic and residential development in the private market. While we view our measure as a useful theoretically-grounded diagnostic tool for policymakers and economists, policy prescriptions ultimately require general equilibrium analysis. Existing quantitative spatial models of commuting could serve as a natural point of departure (e.g., Allen et al., 2015; Ahlfeldt et al., 2015; Monte et al., 2018).[22]

Similarly, our investigation of the relationship between car and transit accessibility and various health and pollution outcomes remains suggestive and does not attempt to compare the economic costs and benefits of accessibility in a systematic and unified manner. While many existing studies estimate the causal effects of a particular type of transportation infrastructure on a specific health outcome (e.g., Gendron-Carrier et al., 2022; Currie and Walker, 2011), no study has attempted a comprehensive assessment of the wide range of costs and benefits of transportation infrastructure interventions. The marginal value of public funds approach (Hendren and Sprung-Keyser, 2020) provides an exciting

---

[21]New Orleans and Dallas face pressure from residents and activists to address the pollution, noise, and safety hazards associated with their mega-roads (New York Times, May 27, 2021).

[22]Applications include an evaluation of the Los Angeles Metro Rail extension (Severen, 2022), measuring the effects of the world's largest bus rapid transit system in Bogotá (Tsivanidis, 2022), and optimal-transportation-system design in general equilibrium frameworks (Fajgelbaum and Schaal, 2020; Allen and Arkolakis, 2022a). Redding and Rossi-Hansberg (2017) provide a general summary of this literature.

framework to combine different causal estimates and map them into exactly such a dollar-denominated cost-benefit analysis.

Lastly, our approach does not account for the monetary costs of different commute modes: transit fares, for example, or parking costs, car maintenance, and insurance. Such costs help drive mode choices; policymakers could employ them as levers to advance cities towards car- or transit-oriented commuting systems.

REFERENCES

ADLER, M. W. AND J. N. VAN OMMEREN (2016): "Does Public Transit Reduce Car Travel Externalities? Quasi-natural Experiments' Evidence from Transit Strikes," *Journal of Urban Economics*, 92, 106–119.

AHLFELDT, G. M., S. J. REDDING, D. M. STURM, AND N. WOLF (2015): "The Economics of Density: Evidence from the Berlin Wall," *Econometrica*, 83, 2127–2189.

AKBAR, P. A., V. COUTURE, G. DURANTON, AND A. STOREYGARD (2021): "Mobility and Congestion in Urban India," Tech. rep., Wharton mimeo.

ALLCOTT, H., R. DIAMOND, J.-P. DUBÉ, J. HANDBURY, I. RAHKOVSKY, AND M. SCHNELL (2019): "Food Deserts and the Causes of Nutritional Inequality," *The Quarterly Journal of Economics*, 134, 1793–1844.

ALLEN, T. AND C. ARKOLAKIS (2022a): "The Welfare Effects of Transportation Infrastructure Improvements," *The Review of Economic Studies*, 89, 2911–2957.

——— (2022b): "The welfare effects of transportation infrastructure improvements," *The Review of Economic Studies*, 89, 2911–2957.

ALLEN, T., C. ARKOLAKIS, AND X. LI (2015): "Optimal City Structure," .

ANDREWS, I., J. STOCK, AND L. SUN (2019): "Weak Instruments in IV Regression: Theory and Practice," *Annual Review of Economics*, 11, 727–753.

BAUM-SNOW, N. (2007): "Did Highways Cause Suburbanization?" *The Quarterly Journal of Economics*, 122, 775–805.

BENTO, A. M., M. L. CROPPER, A. M. MOBARAK, AND K. VINHA (2005): "The effects of urban spatial structure on travel demand in the United States," *Review of Economics and Statistics*, 87, 466–478.

BRUECKNER, J. K. (1987): "The Structure of Urban Equilibria: A Unified Treatment of the Muth-Mills Model," *Handbook of regional and urban economics*, 2, 821–845.

COUTURE, V., G. DURANTON, AND M. A. TURNER (2018): "Speed," *Review of Economics and Statistics*, 100, 725–739.

COUTURE, V., C. GAUBERT, J. HANDBURY, AND E. HURST (2021): "Income Growth and the Distributional Effects of Urban Spatial Sorting," Tech. rep.

COUTURE, V. AND J. HANDBURY (2020): "Urban revival in America," *Journal of Urban Economics*, 119, 103267.

CURRIE, J. AND R. WALKER (2011): "Traffic Congestion and Infant Health: Evidence from E-ZPass," *American Economic Journal: Applied Economics*, 3, 65–90.

DURANTON, G. AND D. PUGA (2015): "Urban Land Use," in *Handbook of Regional and Urban Economics*, Elsevier, vol. 5, 467–560.

DURANTON, G. AND M. A. TURNER (2011): "The Fundamental Law of Road Congestion: Evidence from US Cities," *American Economic Review*, 101, 2616–52.

FAJGELBAUM, P. D. AND E. SCHAAL (2020): "Optimal Transport Networks in Spatial Equilibrium," *Econometrica*, 88, 1411–1452.

GENDRON-CARRIER, N., M. GONZALEZ-NAVARRO, S. POLLONI, AND M. A. TURNER (2022): "Subways and Urban Air Pollution," *American Economic Journal: Applied Economics*, 14, 164–96.

GLAESER, E. L. AND M. E. KAHN (2010): "The Greenness of Cities: Carbon Dioxide Emissions and Urban Development," *Journal of Urban Economics*, 67, 404–418.

HANSEN, W. G. (1959): "How Accessibility Shapes Land Use," *Journal of the American Institute of Planners*, 25, 73–76.

HENDREN, N. AND B. SPRUNG-KEYSER (2020): "A Unified Welfare Analysis of Government Policies," *The Quarterly Journal of Economics*, 135, 1209–1318.

HOLIAN, M. J. AND M. E. KAHN (2012): "The Impact of Center City Economic and Cultural Vibrancy on Greenhouse Gas Emissions from Transportation." Tech. rep., Mineta Transportation Institute.

INGRAM, D. R. (1971): "The Concept of Accessibility: A Search for an Operational Form," *Regional Studies*, 5, 101–107.

KHREIS, H., A. D. MAY, AND M. J. NIEUWENHUIJSEN (2017): "Health Impacts of Urban transport Policy Measures: A Guidance Note for Practice," *Journal of Transport & Health*, 6, 209–227.

KNITTEL, C. R., D. L. MILLER, AND N. J. SANDERS (2016): "Caution, Drivers! Children Present: Traffic, Pollution, and Infant Health," *Review of Economics and Statistics*, 98, 350–366.

KREINDLER, G. (2022): "Peak-hour Road Congestion Pricing: Experimental Evidence and Equilibrium Implications," .

KREINDLER, G., A. GADUH, T. GRAFF, R. HANNA, AND B. A. OLKEN (2023): "Optimal Public Transportation Networks: Evidence from the World's Largest Bus Rapid Transit System in Jakarta," Tech. rep., National Bureau of Economic Research.

LOS ANGELES TIMES, NOVEMBER 11 (2021): "Freeways Force Out Residents in Communities of Color — Again," https://www.latimes.com/projects/us-freeway-highway-expansion-black-latino-communities, [Online Only; accessed 26-October-2022].

MIYAUCHI, Y., K. NAKAJIMA, AND S. J. REDDING (2021): "The economics of spatial mobility: Theory and evidence using smartphone Data," Tech. rep., National Bureau of Economic Research.

MONTE, F., S. J. REDDING, AND E. ROSSI-HANSBERG (2018): "Commuting, Migration, and Local Employment Elasticities," *American Economic Review*, 108, 3855–90.

NEW YORK TIMES, FEB. 11 (2022): "How Billions in Infrastructure Funding Could Worsen Global Warming," https://www.nytimes.com/2022/02/10/climate/highways-climate-change-traffic.html, [Online; accessed 26-October-2022].

NEW YORK TIMES, MAY 27 (2021): "Can Removing Highways Fix America's Cities?" https://www.nytimes.com/interactive/2021/05/27/climate/us-cities-highway-removal.html, [Online Only; accessed 26-October-2022].

OLEA, J. L. M. AND C. PFLUEGER (2013): "A Robust Test for Weak Instruments," *Journal of Business Economic Statistics*, 31, 358–369.

PARRY, I. W., M. WALLS, AND W. HARRINGTON (2007): "Automobile Externalities and Policies," *Journal of Economic Literature*, 45, 373–399.

REDDING, S. J. AND E. ROSSI-HANSBERG (2017): "Quantitative Spatial Economics," *Annual Review of Economics*, 9, 21–58.

SCHLENKER, W. AND W. R. WALKER (2016): "Airports, Air Pollution, and Contemporaneous Health," *The Review of Economic Studies*, 83, 768–809.

SEVEREN, C. (2021): "Commuting, labor, and housing market effects of mass transportation: Welfare and identification," *Review of Economics and Statistics*, 1–99.

——— (2022): "Commuting, Labor, and Housing Market Effects of Mass Transportation: Welfare and Identification," *The Review of Economics and Statistics*, 1–99.

TSIVANIDIS, J. N. (2022): "Evaluating the Impact of Urban Transit Infrastructure: Evidence from Bogotá's TransMilenio," Tech. rep., University of Chicago.

WU, H. AND D. LEVINSON (2020): "Unifying Access," *Transportation Research Part D: Transport and Environment*, 83, 102355.

A. Theory: Derivations and Extensions

A.1 Derivations of Main Model Results

In this section, we derive a more general version of the formula in the main part of the paper that includes many locations of work.

Consider a closed city that consists of an equally-spaced grid of $i = 1, ..., I$ discrete locations and $j = 1, ..., J$ centers of employment. The city is inhabited by $\bar{L} = 1$ workers. Workers can reach centers of employment by commuting via any of $m = 1, ..., M$ modes. Without loss of generality we set the land area in each grid to 1 so that $A_i = 1$. We assume that workers have Cobb-Douglas preferences, spending a fraction α of their income on land and the rest on the homogeneous, freely-traded final good produced in the employment centers whose price serves as the numeraire.

Worker ω chooses a location of residence, commuting mode, and center of employment by solving:

$$\max_{ijm} \frac{w(1 - \tau_{ij}^m)}{r_i^\alpha} \eta_{ij}^m(\omega)$$

where r_i denotes the rent per unit of land and $\eta_{ij}^m(\omega)$ is an idiosyncratic preference shock that we assume to be Fréchet-distributed. We denote by θ the inverse dispersion of idiosyncratic preference shocks. We interpret $1 - \tau_{ij}^m$ as the util-denominated cost of commuting from location i to location j via mode m.

Using standard results in the quantitative spatial economics literature for aggregation in the presence of idiosyncratic heterogeneity that follows an extreme value distribution, the choice probability of home i, work j, and mode m reads

$$\phi_{ij}^m = \frac{w^\theta (1 - \tau_{ij}^m)^\theta r_i^{-\theta\alpha}}{\sum_{i,j,m} w^\theta (1 - \tau_{ij}^m)^\theta r_i^{-\theta\alpha}}$$

Average welfare in the city economy can be written as:

$$u = \Gamma\left(1 - \frac{1}{\theta}\right)\left(\sum_{i,j,m} w^\theta (1 - \tau_{ij}^m)^\theta r_i^{-\theta\alpha}\right)^{\frac{1}{\theta}}.$$

First notice that we can write total welfare as follows:

$$\left(\frac{u}{\Gamma(1 - \frac{1}{\theta})}\right)^\theta = \sum_{i,m} w^\theta (1 - \tau_{ij}^m)^\theta r_i^{-\theta\alpha} + \sum_{i,k \neq j,m} w^\theta (1 - \tau_{ik}^m)^\theta r_i^{-\theta\alpha}.$$

But then

$$\left(\frac{u}{\Gamma(1 - \frac{1}{\theta})}\right)^\theta = \sum_{i,m} w^\theta (1 - \tau_{ij}^m)^\theta r_i^{-\theta\alpha} + \left(\frac{u}{\Gamma(1 - \frac{1}{\theta})}\right)^\theta \sum_{i,k \neq j,m} \phi_{ik}^m$$

so that:

$$\tilde{u} := \left(\frac{u}{\Gamma(1 - \frac{1}{\theta})}\right)^\theta = \frac{1}{\phi_j}\sum_{i,m} w^\theta (1 - \tau_{ij}^m)^\theta r_i^{-\theta\alpha}$$

where ϕ_j is the share of all employment in the economy that occurs in location j. From now on, we refer to location j as the CBD. In the model presented in the paper, $\phi_j = 1$ by assumption. We also defined a useful monotonic transformation of welfare in the city, $\tilde{u}$.

Next, consider land market clearing in location i:

$$r_i A_i = \alpha w \sum_{j,m} \phi_{ij}^m = \alpha w \frac{\sum_{j,m} w^\theta (1 - \tau_{ij}^m)^\theta r_i^{-\theta\alpha}}{\sum_{i,j,m} w^\theta (1 - \tau_{ij}^m)^\theta r_i^{-\theta\alpha}} = \alpha w^{1+\theta} r_i^{-\theta\alpha} \tilde{u}^{-1} \sum_{j,m} (1 - \tau_{ij}^m)^\theta$$

We can solve the land market clearing equation for rent:

$$r_i = \alpha^{\frac{1}{1+\theta\alpha}} w^{\frac{1+\theta}{1+\theta\alpha}} \tilde{u}^{-\frac{1}{1+\theta\alpha}} A_i^{-\frac{1}{1+\theta\alpha}} \left[\sum_{j,m} (1 - \tau_{ij}^m)^\theta\right]^{\frac{1}{1+\theta\alpha}}$$

But then we can plug this expression into the expression for welfare:

$$\tilde{u} = \frac{1}{\phi_j}\sum_{i,m} w^\theta (1 - \tau_{ij}^m)^\theta \alpha^{\frac{-\theta\alpha}{1+\theta\alpha}} w^{\frac{-\theta\alpha(1+\theta)}{1+\theta\alpha}} \tilde{u}^{\frac{\theta\alpha}{1+\theta\alpha}} A_i^{\frac{\theta\alpha}{1+\theta\alpha}} \left[\sum_{j,m} (1 - \tau_{ij}^m)^\theta\right]^{\frac{-\theta\alpha}{1+\theta\alpha}}$$

Collecting terms and re-arranging:

$$\alpha^{\frac{\theta\alpha}{1+\theta\alpha}}\tilde{u}^{1-\frac{\theta\alpha}{1+\theta\alpha}} = \frac{1}{\phi_j}w^{\theta(1-\frac{\alpha(1+\theta)}{1+\theta\alpha})}\sum_{i,m}\frac{(1-\tau_{ij}^m)^\theta}{\left[\sum_{j,m}(1-\tau_{ij}^m)^\theta\right]^{\frac{\theta\alpha}{1+\theta\alpha}}}A_i^{\frac{\theta\alpha}{1+\theta\alpha}}$$

Notice that we can write:

$$\frac{(1-\tau_{ij}^m)^\theta}{\left[\sum_{j,m}(1-\tau_{ij}^m)^\theta\right]^{\frac{\theta\alpha}{1+\theta\alpha}}} = \frac{(1-\tau_{ij}^m)^{\theta\frac{\theta\alpha}{1+\theta\alpha}}}{\left[\sum_{j,m}(1-\tau_{ij}^m)^\theta\right]^{\frac{\theta\alpha}{1+\theta\alpha}}}(1-\tau_{ij}^m)^{\theta(1-\frac{\theta\alpha}{1+\theta\alpha})} = (\psi_{ij}^m)^{\frac{\theta\alpha}{1+\theta\alpha}}(1-\tau_{ij}^m)^{\theta(1-\frac{\theta\alpha}{1+\theta\alpha})}$$

where ψ_{ij}^m is the share of all residents in location i that commutes to destination j via mode m. Defining $\iota = \theta(1 - \frac{\theta\alpha}{1+\theta\alpha}) > 0$, we hence obtain the following expression for welfare,

$$\bar{u} := \alpha^{1-\frac{\iota}{\theta}}\tilde{u}^{\frac{\iota}{\theta}} = \frac{1}{\phi_j}w^{\iota\frac{1+\theta}{\theta}-1}\sum_{i,m}(\psi_{ij}^m)^{1-\frac{\iota}{\theta}}(1-\tau_{ij}^m)^\iota A_i^{1-\frac{\iota}{\theta}},$$

where ι measures the importance of housing prices and commuting times, relative to the strength of idiosyncratic motives for location choices. The term $\bar{u}$ represents another monotonic transformation of welfare in the model.

We now assume there are discrete commuting costs indexed by κ and denote the commuting cost associated with κ by $\tau_j(\kappa)$. Recall that all locations have the same area, $A_i = 1$. Now we collect locations with the same commuting distance to destination j via a given mode m. Denote the set of all locations i from which j can be reached with a commuting cost indexed by κ via mode m by $\Lambda_j^m(\kappa)$. We can now sum across i within the same-commute-cost set $\Lambda_j^m(\kappa)$ to obtain:

$$\bar{u} = \frac{1}{\phi_j}w^{\iota\frac{1+\theta}{\theta}-1}\sum_{\kappa,m}(1-\tau_j(\kappa))^\iota\frac{\mid\Lambda_j^m(\kappa)\mid}{\mid\Lambda_j^m(\kappa)\mid}\sum_{i\in\Lambda_j^m(\kappa)}(\psi_{ij}^m)^{1-\frac{\iota}{\theta}} = \frac{1}{\phi_j}w^{\iota\frac{1+\theta}{\theta}-1}\sum_{\kappa,m}(1-\tau_j(\kappa))^\iota\mathcal{A}_j^m(\kappa)\bar{\psi}_j^m(\kappa)$$

where $\mathcal{A}_j^m(\kappa) = \mid\Lambda_j^m(\kappa)\mid$ is the total land area associated with commuting costs κ via mode m to the destination j which is equal to the total number of locations that offer this commuting time. We define:

$$\bar{\psi}_j^m(\kappa) = \frac{1}{\mid\Lambda_j^m(\kappa)\mid}\sum_{i\in\Lambda_j^m(\kappa)}(\psi_{ij}^m)^{1-\frac{\iota}{\theta}}$$

which is the (transformed) fraction of residents in $\mathcal{A}_j^m(\kappa)$ that commute to destination j using mode m.

The equation we present in the main part of the paper is a special case of the above result with a single destination j. In this case $\phi_j = 1$ and we drop the j indexing so that:

$$\bar{u} = w^{\iota \frac{1+\theta}{\theta}-1} \sum_{\kappa, m} (1 - \tau(\kappa))^\iota \mathcal{A}^m(\kappa) \bar{\psi}^m(\kappa).$$

A.2   Housing Supply vs. Land Supply

In the main version of the model, we assume that workers consume land directly. In reality, workers consume housing. We can replace land in the above model with housing supply H_i and choose locations i such that they all have the same housing supply. Then we obtain

$$\bar{u} = w^{\iota \frac{1+\theta}{\theta}-1} \sum_{\kappa, m} (1 - \tau(\kappa))^\iota \mathcal{H}^m(\kappa) \bar{\psi}^m(\kappa),$$

where we denote by $\mathcal{H}^m(\kappa)$ the housing supply within a commute time κ from the CBD on mode m. We can re-introduce land area by writing

$$\bar{u} = w^{\iota \frac{1+\theta}{\theta}-1} \sum_{\kappa, m} (1 - \tau(\kappa))^\iota \bar{\psi}^m(\kappa) \frac{\mathcal{H}^m(\kappa)}{\mathcal{A}^m(\kappa)} \mathcal{A}^m(\kappa),$$

where $\frac{\mathcal{H}^m(\kappa)}{\mathcal{A}^m(\kappa)}$ measures the density of housing development and $\mathcal{A}^m(\kappa)$, as before, denotes the land area from which the CBD can be reached in a commute time κ via mode m.

A.3   A Housing Sector

Consider a model in which consumer have preferences over housing services. This amounts to replacing land supply A_i with housing supply H_i in the baseline version of our model.

Suppose there exists a competitive housing sector which transforms the final good and land into housing services, H_i, using the following production function:

$$H_i = q^\zeta a^{1-\zeta},$$

where q denotes the amount of the final good used and a denotes the amount of land used in production. If we denote the price of land in location i by p_i, we can write the first order conditions of the firm as:

$$r_i \zeta q^{\zeta-1} a^{1-\zeta} = 1 \quad \text{and} \quad r_i(1-\zeta)q^{\zeta}a^{-\zeta} = p_i$$

Combining and plugging into the zero profit condition yields:

$$q = r_i^{\frac{1}{1-\zeta}} a \zeta^{\frac{1}{1-\zeta}}$$

Using land market clearing which implies $a_i = A_i$, we then obtain an equation for equilibrium housing supply:

$$H_i = r_i^{\frac{\zeta}{1-\zeta}} \zeta^{\frac{\zeta}{1-\zeta}} A_i$$

But recall that we have an expression for rents in each location:

$$r_i = \alpha^{\frac{1}{1+\theta\alpha}} w^{\frac{1}{1+\theta\alpha}} \tilde{u}^{-\frac{1}{1+\theta\alpha}} H_i^{-\frac{1}{1+\theta\alpha}} \left(\sum_{j,m}(1-\tau_{ij}^m)^{\theta}\right)^{\frac{1}{1+\theta\alpha}}$$

But then we can solve for rents in terms of land:

$$r_i^{1+\frac{1}{1+\theta\alpha}\frac{\zeta}{1-\zeta}} = \alpha^{\frac{1}{1+\theta\alpha}} w^{\frac{1}{1+\theta\alpha}} \tilde{u}^{-\frac{1}{1+\theta\alpha}} \zeta^{-\frac{1}{1+\theta\alpha}\frac{\zeta}{1-\zeta}} A_i^{-\frac{1}{1+\theta\alpha}} \left(\sum_{j,m}(1-\tau_{ij}^m)^{\theta}\right)^{\frac{1}{1+\theta\alpha}}$$

We can then solve for r_i and plug the rental rate into our expression for welfare:

$$\tilde{u} = \frac{1}{\phi_j}\sum_{i,m} w^{\theta}(1-\tau_{ij}^m)^{\theta} r_i^{-\theta\alpha}$$

to obtain a similar expression as the one in the paper of welfare in terms of land area at different commuting cost distances from the CBD.

A.4 The Monocentric City Model

Consider the basic closed-city monocentric city model with one type of commuting mode and one CBD. There is a mass $\bar{L}$ of workers. Workers choose their location i, their consumption of the final good (c), and their consumption of

housing (h) to maximize:

$$\max_{c,h,i} u(c,h) \quad \text{s.t.} \quad c + r_i h = w - \tau_i$$

where τ_i is the commuting cost in dollars to the CBD from location i and r_i is the rent per unit of land. We assume that utility takes the Cobb-Douglas form so that:

$$u(c,h) = c^{1-\alpha} h^{\alpha}.$$

There are no idiosyncratic preferences. In spatial equilibrium, utility must be equalized across all inhabited locations to some value $\bar{u}$, so that:

$$u = u_i = \frac{w - \tau_i}{r_i^{\alpha}}$$

where the consumption good serves as numeraire. Now consider land market clearing:

$$r_i = A_i^{-1} \alpha L_i (w - \tau_i),$$

where L_i denotes the equilibrium number of workers in location i and A_i the supply of land in location i. We can plug this into the expression for equilibrium utility to obtain:

$$u = A_i^{\alpha} \alpha^{-\alpha} L_i^{-\alpha} (w - \tau_i)^{1-\alpha}$$

Now we can solve for the number of people and sum across all inhabited locations (which is an equilibrium outcome itself):

$$L_i = u^{-\frac{1}{\alpha}} A_i \alpha^{-1} (w - \tau_i)^{\frac{1-\alpha}{\alpha}} \Rightarrow \bar{L} = u^{-\frac{1}{\alpha}} \alpha^{-1} \sum_i A_i (w - \tau_i)^{\frac{1-\alpha}{\alpha}}$$

But then we can solve for city welfare:

$$u = \bar{L}^{-\alpha} \alpha^{-\alpha} \left(\sum_i (w - \tau_i)^{\frac{1-\alpha}{\alpha}} A_i \right)^{\alpha},$$

but then, as in the model in the main part of the paper, more land in location with lower commuting costs raises welfare the most. Also notice that more people lower city utility because areas around the CBD get more expensive.

B. Alternative Measurement Approaches

There are several ways to construct accessibility zones in the data. In the body of the paper, we rely on proprietary software, namely the Isochrone API from TravelTime Technologies (https://app.traveltime.com/), which automates the construction process. Other companies offer the same service, and constructing accessibility zones from first principles is possible using any route-finding API.

Table B.1: Pairwise Correlations among Accessibility-Zone Areas

Source	Traveltime	Targomo	Google Maps
Traveltime	1.00	-	-
Targomo	0.71	1.00	-
Google Maps	0.84	0.77	1.00

Notes: The table compares the (0,60)-minute car accessibility-zone areas computed using three different approaches for the 27 largest US and 25 largest European cities. All accessibility-zone areas are for commutes that arrive in the CBD at 8:45 AM on a Wednesday. The different computing approaches include using the proprietary software of TravelTime Technologies (Row 1) or Targomo (Row 2) as well as using Python and the Google Maps API to construct the zones ourselves (Row 3).

Table B.1 shows the correlations between the (0,60)-minute car accessibility-zone areas from TravelTime and the same areas computed using (i) an alternative software provider, Targomo (https://www.targomo.com), as well as (ii) Python combined with optimal routes obtained from Google Maps. The correlations are high: all three sources deliver comparable estimates of the accessibility-zone areas.

C. Accessibility, Infrastructure, and Mode Choices

In this section, we examine the correlations between our accessibility-zone areas and traditional measures of infrastructure (e.g., road length) as well as the actual mode choices of commuters.

Accessibility and Infrastructure.   Table C.1 shows coefficient estimates from a regression of (0,60)-minute accessibility-zone areas in the US and Europe on traditional measures of transportation infrastructure, separately for public transit and cars. We include a constant and a control for city population size in all regressions. The pooled regression also includes a Europe dummy.

As expected, the public transit accessibility-zone area and the number of rail miles positively correlate in the US and Europe. Similarly, car accessibility and total street miles are strongly positively correlated in the US. The same correlation is less strong and insignificant in Europe, perhaps reflecting that large street networks in old European city centers were not designed for cars: large cities with a lot of streets have smaller accessibility zones relative to quantity of infrastructure since their cores are so hard to navigate. Road length in the US also correlates positively with the size of public transit accessibility zones, perhaps because transit systems in many US cities, unlike in Europe, rely primarily on buses.

TABLE C.1: ACCESSIBILITY ZONES AND INFRASTRUCTURE

log of...	United States		Europe		Pooled	
	$\mathcal{A}^P_{0,60}$	$\mathcal{A}^C_{0,60}$	$\mathcal{A}^P_{0,60}$	$\mathcal{A}^C_{0,60}$	$\mathcal{A}^P_{0,60}$	$\mathcal{A}^C_{0,60}$
Rail Miles	0.0584**	-0.0460	0.149**	0.0594	0.0942***	0.0273
	(0.0264)	(0.0394)	(0.0670)	(0.0749)	(0.0270)	(0.0378)
Street Miles	0.564**	0.940***	0.122	0.359	0.381*	0.590**
	(0.224)	(0.203)	(0.302)	(0.447)	(0.196)	(0.251)
Observations	52	52	51	51	103	103
R-squared	0.647	0.302	0.351	0.122	0.613	0.265

Notes: All regressions regress log accessibility-zone areas on log measures of transportation infrastructure. All regressions include a constant term and a control for OECD metro area population; the pooled regressions include a Europe dummy. We add 1 to the total rail miles in each city. Robust standard errors in parentheses. *** $p<0.01$, ** $p<0.05$, * $p<0.1$. We present a complete list of data sources in Appendix Table D.5.

Accessibility and Transportation-Mode Choice.   Table C.2 regresses mode shares for driving, public transit, and non-motorized commutes on our accessibility measures. The mode shares are the fraction of workers commuting into the CBD using a particular mode. As expected, in cities with larger driving accessibility zones, more people use cars to get to work, and fewer people use public

transit. Likewise, in cities with larger public transit accessibility zones, more people use public transit for their commutes, and fewer people use cars.

Interestingly, public transit accessibility areas are also positively correlated with the walk/bike mode share. By contrast, larger car accessibility areas negatively correlate with the use of these modes, although this relationship is not significant. These differences in correlations suggest that cities with more public transit and less car infrastructure are more walkable, which could explain some of the external costs of car orientation discussed in Section 4. European workers are substantially less likely than US workers to commute by car; instead, they display similarly higher propensities to take public transit or walk/bike to work. Finally, workers in large cities are more likely to use public transit.

TABLE C.2: ACCESSIBILITY ZONES AND MODE SHARES

	Share of CBD Commutes via		
	Driving	Transit	Walk+Bike
$\log \mathcal{A}^P_{0,60}$	-0.186***	0.145***	0.0353*
	(0.0351)	(0.0350)	(0.0197)
$\log \mathcal{A}^C_{0,60}$	0.0722***	-0.0392**	-0.0318
	(0.0214)	(0.0194)	(0.0207)
log Population	-0.0550	0.0588*	-0.00194
	(0.0349)	(0.0345)	(0.0141)
Europe Dummy	-0.182***	0.0794***	0.108***
	(0.0335)	(0.0300)	(0.0170)
Observations	96	96	98
R-squared	0.754	0.632	0.586

Notes: All regressions include a constant term, which we do not report. Robust standard errors in parentheses. *** p<0.01, ** p<0.05, * p<0.1. We present a complete list of data sources in Appendix Table D.5. Note the mode shares across Driving, Transit, and Walk+Bike do not sum to 1, due to the "Other" category in data.

D. ADDITIONAL FIGURES AND TABLES

In this section, we present additional Figures and Tables.

In our main measurement exercise, we constructed accessibility zones for a single CBD. In reality, many cities have several centers of employment. Table D.1 shows summary statistics for an alternative set of *polycentric* accessibility zones. In particular, we use ZIP code level data on total payroll to compute the payroll density, i.e. per square kilometer, of each ZIP code (as a proxy for the amount of economic activity per square meter) and then define the employment centers of a city as the collection of the highest-payroll-density ZIP codes that collectively account for 10 % of a city's total payroll. We then compute accessibility zones for each of these employment-center ZIP codes' centroids; our polycentric accessibility zones are then the spatial union of all individual employment centers' accessibility zones. This procedure generates the total area from which any of these ZIP codes can be reached within $(t, t + \Delta)$ minutes.

In an additional robustness check, we allow for park and ride as a third option beyond pure public transit or car commutes. TravelTime's Isochrone API includes a "driving+train" mode option for the US and UK which simulates trips that may involve, in addition to rail transit, up to some maximum threshold number of minutes of driving at the beginning, but not end, of the trip. The driving segment must end at a public parking lot, and the rest of the trip must be completed via some combination of rail transit and walking, thus excluding buses. The algorithm accounts for the time spent parking and transferring to the train, and the rail transit portion allows all rail-based modes such as heavy rail subway, light rail, or commuter rail. "Driving+train" thus provides a realistic approximation of the gains from combining modes in a feasible fashion. In order to further mimic the behavior of actual park-and-ride users, we set the maximum driving threshold to 15 minutes.[23]

In Figure D.1, we plot the park-and-ride (driving plus train) accessibility zone area against those for pure public transit (train and bus only) for the (15,30)- and (45,60)-minute intervals. Most US cities lack a rail transit option to enable park and ride, and even cities with rail may have few stations so close to the CBD. Since our park-and-ride option does not permit bus travel, the associated (15,30)-minute accessibility-zone areas in most cities are actually much smaller than for bus+train. In contrast, the driving+train accessibility zone areas in cities with robust rail systems often substantially exceed their pure public transit counterparts. Table D.2 lists the US and UK cities where the (45,60)-minute driving+train accessibility zone area exceeds the (45,60)-minute pure

---

[23]Note that, due to the vastly larger size of the car accessibility zones, allowing unlimited driving as part of the driving+train mode simply reproduces the driving accessibility zones.

FIGURE D.1: DRIVING+TRAIN VS. PUBLIC TRANSIT ACCESSIBILITY ZONE
AREAS IN THE US

(A) $\mathcal{A}^m_{15,30}$ (B) $\mathcal{A}^m_{45,60}$
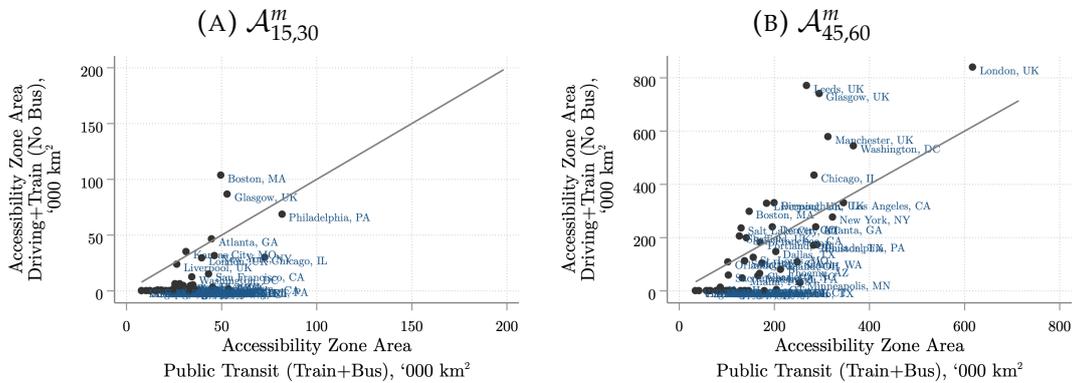
Notes: This figure shows scatter plots of driving+train accessibility zone areas, which allow up to 15 minutes of driving plus rail transit (e.g. subway or commuter rail, but *not* bus), versus public transit accessibility zone areas (which allow bus and train use) on a Wednesday at 8:45 AM and for the (15,30)- and (45,60)-minute commute time intervals. Both panels also include a 45-degree line for reference.

public transit (bus+train) area, along with the corresponding accessibility-zone areas for driving+train ("D+T") and pure public transit ("P").

Table D.3 supplements Section 3.5 and provides the average share of total OECD metro area population that lives in each accessibility zone. Because we use total metro area populations from the OECD, shares can add up to more than one if accessibility zones extend beyond the scope of OECD-defined metro area boundaries.

Figure D.2 presents a graphic taken from Khreis et al. (2017), which diagrammatically shows the linkages between urban transport policy and planning, and adverse health impacts. The figure helped us select variables to analyze in Section 4 in the main text. Table D.4 presents the OLS versions of the IV specifications discussed in Table 6 in the main text.

Table D.5 provides the data source and unit of measurement of every variable used in the paper. Similarly, Table D.6 provides summary statistics of all the variables used throughout the paper.

Tables D.7 and D.8 list the (0,15)-, (15,30)-, (30,45)-, and (45,60)-minute accessibility-zone areas for every US and European city in our sample, separately for driving and public transit.

TABLE D.1: MONOCENTRIC VS. POLYCENTRIC ACCESSIBILITY ZONES IN THE US

	Car		Public Transit		Car/Public Transit	
Panel A: Area						
	Monocentric	Polycentric	Monocentric	Polycentric	Monocentric	Polycentric
0-15	85.94	170.16***	3.86	7.72***	26.84	25.94
15-30	725.95	928.78***	29.70	38.02**	31.04	37.76
30-45	1493.27	1701.15***	91.18	109.20***	18.85	20.04
45-60	2260.38	2454.55***	149.93	171.14***	19.22	19.68
Panel B: Population Share						
	Monocentric	Polycentric	Monocentric	Polycentric	Monocentric	Polycentric
0-15	0.08	0.13***	0.005	0.009***	23.74	37.02
15-30	0.35	0.39***	0.04	0.04	15.36	27.79
30-45	0.31	0.31	0.078	0.084*	5.14	4.69
45-60	0.22	0.25	0.10	0.10	2.61	2.58

Notes: This table shows average US accessibility-zone areas (Panel A) and shares of OECD metro area population (Panel B) for various time intervals and modes on a Wednesday at 8:45 AM, computed using our monocentric CBDs as well as a polycentric robustness check, where we take the union of accessibility-zone areas of the top zip codes by payroll density in the metro area. The "Car/Public Transit" panel shows averages of the ratio of the car relative to public transit accessibility-zone areas or population shares for each accessibility zone type and time interval. We conducted paired two-sided t-tests for the difference in means of each set of monocentric vs. polycentric measures; the number of stars indicates the p-value with the following interpretation: *** $p<0.01$, ** $p<0.05$, * $p<0.1$.

TABLE D.2: CITIES WHERE 45-60 MINUTE DRIVING+TRAIN DOMINATES
PUBLIC TRANSIT

City	$\mathcal{A}^{P}_{15,30}$	$\mathcal{A}^{D+T}_{15,30}$	$\mathcal{A}^{P}_{45,60}$	$\mathcal{A}^{D+T}_{45,60}$
London, UK	39.74	28.94	618.0	837.7
Leeds, UK	33.12	0.125	268.9	768.8
Glasgow, UK	53.22	86.49	294.7	739.4
Manchester, UK	28.07	5.850	313.8	576.5
Washington, DC	34.59	11.97	367.0	542.8
Chicago, IL	72.79	29.56	284.0	432.9
Birmingham, UK	29.81	0.534	200.0	330.0
Liverpool, UK	26.60	23.38	184.5	327.1
Boston, MA	49.80	103.2	147.6	296.5
Denver, CO	31.98	0.110	197.3	239.0
Salt Lake City, UT	25.27	1.963	131.1	235.2
Sheffield, UK	35.90	0.932	127.8	205.2
San Francisco, CA	43.50	14.86	142.0	198.2
Portland, OR	33.85	4.421	171.8	181.2
Orlando, FL	12.47	0	102.9	107.7

Notes: The table lists cities whose 45-60 minute accessibility zone is larger via driving+train (which allows up to 15 minutes of driving plus rail transit, e.g. subway or commuter rail, but *not* bus) than via public transit (train+bus), along with the (15,30)- and (45,60)-minute accessibility zone areas for each mode. Cities in order of decreasing 45-60 minute driving+train area. The areas have been constructed for Wednesday at 8:45 AM. The areas are computed using TravelTime Technologies's Isochrone API.

TABLE D.3: AVERAGE ACCESSIBILITY-ZONE POPULATION SHARE BY REGION
AND MODE
(OF METRO AREA POPULATION)

Min.	Car			Public Transit			Car/Public Transit		
	US	Europe	Ratio	US	Europe	Ratio	US	Europe	Ratio
0-15	0.08	0.08	0.99	0.01	0.03	0.16***	23.74	3.95	6.01**
15-30	0.35	0.35	1.00	0.04	0.18	0.19***	15.36	2.57	5.98
30-45	0.31	0.41	0.76***	0.08	0.23	0.33***	5.14	1.85	2.77
45-60	0.22	0.42	0.52***	0.10	0.22	0.45***	2.61	1.88	1.39

Notes: This figure shows average accessibility-zone population shares, out of total OECD metro area population, for various time intervals and modes in the US and Europe. The third column in the "Car" and "Public Transit" panels shows the ratio of the preceding two numbers in the respective row. The "Car/Public Transit" panel shows averages, across cities, of the ratio of the car relative to public transit accessibility-zone population shares for each time interval and region. The last panel's third column shows the ratio of US cities' mean relative car to transit accessibility-zone population share to the corresponding figure for Europe. We conducted Wald tests in all columns with a "Ratio" header for the null hypothesis that the ratio equals 1. The number of stars indicates the p-value with the following interpretation: *** $p<0.01$, ** $p<0.05$, * $p<0.1$.

FIGURE D.2: OVERVIEW OF TRANSPORTATION POLICY EXTERNALITIES
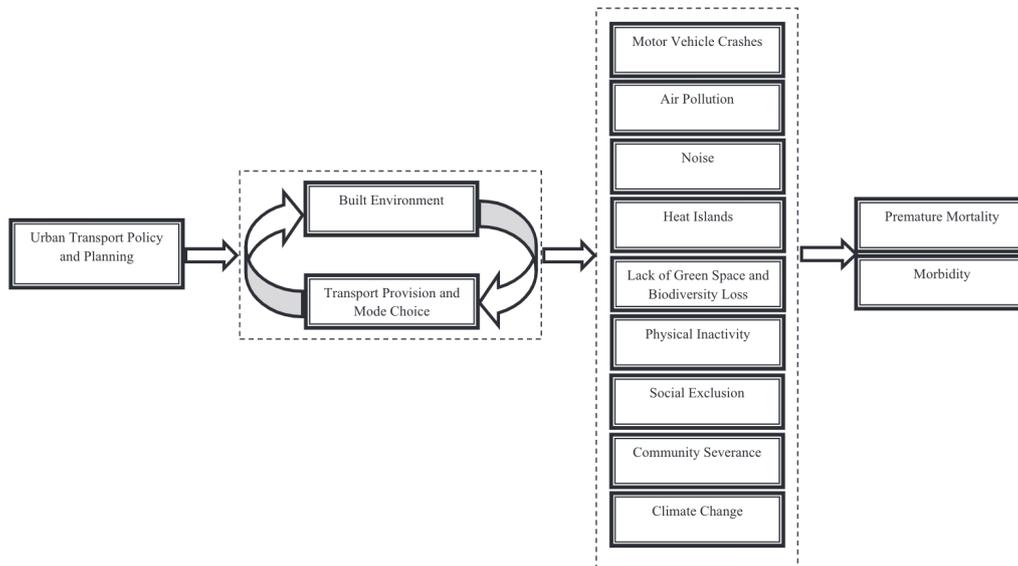
Notes: This figure shows Figure 1 from Khreis et al. (2017), which in their paper was entitled "Linkages between Urban Transport and Adverse Health Impacts."

TABLE D.4: THE COSTS OF ACCESSIBILITY: OLS EQUIVALENTS OF IV
SPECIFICATIONS

Panel A: Land Use

	Log Total km per km^2			Green-space	Walking
	Motorway	Streets	Bike Lanes	per km^2	Index
$\log\left(\mathcal{A}_{0,60}^C/\mathcal{A}_{0,60}^P\right)$	0.288***	0.0872	0.103	-0.0645**	-0.876***
	(0.100)	(0.0610)	(0.383)	(0.0283)	(0.307)

Panel B: Direct Health Externalities

	Share Physically	Sh. Poor + Far from	Share	Deaths per 1000	
	Inactive	Groceries	Obese	Traffic	Obesity
$\log\left(\mathcal{A}_{0,60}^C/\mathcal{A}_{0,60}^P\right)$	0.0170**	0.0184***	0.0209***	0.236*	0.353*
	(0.00681)	(0.00472)	(0.00594)	(0.130)	(0.190)

Panel C: Pollution Externalities

	t/yr			log Mean	Aug. Temp
	$\log CO_2$	$\log NOx$	$\log PM2.5$	Noise	p90/p10
$\log\left(\mathcal{A}_{0,60}^C/\mathcal{A}_{0,60}^P\right)$	0.216***	0.253**	0.176	0.00174	-0.0217
	(0.0635)	(0.102)	(0.113)	(0.00260)	(0.0247)

Panel D: Indirect Health Externalities

	Deaths per 1000			Premature	log Life
	Asthma	COPD	Total	Deaths/100k	Expectancy
$\log\left(\mathcal{A}_{0,60}^C/\mathcal{A}_{0,60}^P\right)$	0.0545	1.501**	-0.000196	0.0368	-0.00560
	(0.0517)	(0.590)	(3.548)	(0.0294)	(0.00379)

Notes: Each regression controls for OECD metro area population. Robust standard errors in parentheses. *** p<0.01, ** p<0.05, * p<0.1. All regressions use 51 of our 52 largest US cities, due to missing data on the instrument for Las Vegas; the motorway and street length specifications also omit Los Angeles.

TABLE D.5: DATA SOURCES

Variable	Unit	Description	Source
Demographics and Economic			
Metro Area population	Count	Population of corresponding OECD metro area	OECD
Urban share of the population	Proportion	Share of population living in urban areas, 2010	NHGIS Table H7W (Census 2010)
Share of employment in manufacturing	Proportion	Share of employment in NAICS codes 31-33, 2015	County Business Patterns
65+-year-olds	Proportion	Share of population aged 65+	NHGIS Table H76 (Census 2010)
Owner-occupied fraction	Proportion	Share of occupied housing units owner-occupied, 2006-2010	NHGIS Table JRK (2006-2010 ACS)
Population Density	Persons per km^2	Population per square kilometer, 2010	NHGIS Table H7X (Census 2010)
Income per capita	$	Per capita income in the past 12 months, 2006-2010	NHGIS Table JQB (2006-2010 ACS)
Share of black residents	Proportion	Share of population Black or African American alone	NHGIS Table H7X (Census 2010)
Share of hispanic residents	Proportion	Share of population Hispanic or Latino	NHGIS Table H7Y (Census 2010)
Mean democratic vote share	Proportion	Mean vote share of democratic presidential candidates, 2000-2016	MIT Election Data + Science Lab
Agricultural share of employment	Proportion	Share of employment in NAICS code 11, 2015	County Business Patterns
Commuters by Mode from Tract to Tract			
Infrastructure and Land Use			
Total street length	kilometer	Used OpenStreetMap API to count total street length within each metro area	OpenStreetMap
Total motorway length	kilometer	Used OpenStreetMap API to count total motorway length within each metro area	OpenStreetMap
Total Bike Lanes length	kilometer	Used OpenStreetMap API to count total bike lane length within each metro area	OpenStreetMap
Greenspace area	Proportion	Share area covered by parks	OpenStreetMap
Pollution			
CO2	Tons	Total annual on-road CO2 emissions	EPA National Emissions Inventory (2017)
NOX	Tons	Total annual on-road NOX emissions	EPA National Emissions Inventory (2017)
PM 2.5	Tons	Total annual on-road PM 2.5 emissions	EPA National Emissions Inventory (2017)
Noise	Decibels	Noise energy emitted from transportation sources over a 24-hour period, averaged over receptor locations within grid cell	National Transportation Noise Mapping Tool
90th/10th percentile August temperature	Ratio	Ratio of 90th to 10th percentile grid-cell-level August temperature (2019)	MODIS Land Surface Temperature and Emissivity (MOD11)
Mean January temperature	Degrees Celsius	Mean grid-cell-level January temperature (2019)	MODIS Land Surface Temperature and Emissivity (MOD11)
Health			
Residents with heavy drinking habits	Proportion	Share of adults reporting binge or heavy drinking.	2020 County Health Rankings
Residents who are smokers smokers	Proportion	Share of adults who are current smokers.	2020 County Health Rankings
Walking Index	Index (1-20)	Composite index of street intersection density, proximity to transit stops, and diversity of land uses	EPA National Walkability Index
Share Physically Inactive	Proportion	Share of adults age 20 and over reporting no leisure-time physical activity	2020 County Health Rankings
Share poor and far from groceries	Proportion	Share of population with income $< 2\times$ poverty line and live > 1 mi. from grocery store	2020 County Health Rankings
Share obese	Proportion	Share of (age 20+) population with BMI¿30 kg/m2	2020 County Health Rankings
Death			
Total Deaths	Deaths/1000 residents	All deaths	CDC Multiple Cause of Death 1999-2019
Traffic Deaths	Deaths/1000 residents	Transport accident deaths according to International Classification of Diseases	CDC Multiple Cause of Death 1999-2019
Obesity Deaths	Deaths/1000 residents	Obesity-caused deaths according to International Classification of Diseases	CDC Multiple Cause of Death 1999-2019
Asthma Deaths	Deaths/1000 residents	Asthma-caused deaths according to International Classification of Diseases	CDC Multiple Cause of Death 1999-2019
COPD Deaths	Deaths/1000 residents	Chronic obstructive pulmonary disease-caused deaths according to International Classification of Diseases	CDC Multiple Cause of Death 1999-2019
Premature Deaths	Years/100k population	Years of potential life lost before age 75 per 100,000 population	2020 County Health Rankings
Life Expectancy	Years	Average number of years a person can expect to live	2020 County Health Rankings

Notes: This table presents a description, the unit of measurement, and the source for every empirical variable used in the paper.

TABLE D.6: SUMMARY STATISTICS

Variable	Aggregation	Unit	Mean	Standard Deviation	Min	Max
Demographics and Economic						
(Total) Metro Area population	County	Persons	3016273	4335979	251446	19961045
Urban share of the population	County	Proportion	0.41	0.31	0	1
Share of employment in manufacturing	County	Proportion	0.15	0.12	0	0.75
65+-year-olds	County	Proportion	0.16	0.04	0.04	0.43
Owner-occupied fraction	County	Proportion	0.73	0.08	0.21	0.91
Population Density	County	Persons per km^2	98.66	661.70	0.05	26544.42
Income per capita	County	$	22452.07	5370.60	7772.00	64381.00
Share of black residents	County	Proportion	0.09	0.15	0.00	0.86
Share of hispanic residents	County	Proportion	0.08	0.13	0.00	0.96
Mean democratic vote share	County	Proportion	0.38	0.13	0.07	0.90
Agricultural share of employment	County	Proportion	0.01	0.02	0	0.35
Commuters by Mode from Tract to Tract						
Infrastructure and Land Use						
Total street length	County	kilometers	2611.85	2174.43	0.00	37046.48
Total motorway length	County	kilometers	85.75	159.39	0.00	2650.58
Total Bike Lanes length	County	kilometers	16.82	106.99	0.00	3734.72
Greenspace area	County	Proportion	0.09	0.17	0	1
Pollution						
CO2	County	Tons	465.38	1440.33	1.39	42337.96
NOX	County	Tons	0.84	1.91	0.01	45.55
PM 2.5	County	Tons	0.04	0.12	0.00	3.86
Noise	County	Decibels	53.57	1.63	45.32	56.96
90th/10th percentile August temperature	County	Ratio	1.13	0.14	1.00	2.17
Mean January temperature	County	Degrees Celsius	2.64	8.21	-20.42	23.19
Health						
Residents with heavy drinking habits	County	Proportion	0.17	0.03	0.08	0.29
Residents who are smokers smokers	County	Proportion	0.17	0.04	0.06	0.41
Walking Index	County	Index (1-20)	6.49	1.92	2.86	16.00
Share Physically Inactive	County	Proportion	0.27	0.06	0.10	0.50
Share poor and far from groceries	County	Proportion	0.09	0.08	0.00	0.72
Share obese	County	Proportion	0.33	0.05	0.12	0.58
Death						
COPD Deaths per 1000	County	Deaths/1000 residents	23.74	8.99	1.04	64.08
Total Deaths	County	Deaths/1000 residents	216.89	53.40	40.33	440.01
Traffic Deaths per 1000	County	Deaths/1000 residents	2.43	1.26	0.30	13.06
Obesity Deaths per 1000	County	Deaths/1000 residents	2.30	1.08	0.30	9.68
Asthma Deaths per 1000	County	Deaths/1000 residents	0.76	0.45	0.14	8.46
Premature Deaths	County	Years/100k population	8525.83	2765.87	2730.60	43939.07
Life Expectancy	County	Years	77.45	3.01	61.63	104.74

Notes: This table presents summary statistics and the spatial unit of measurement for every empirical variable used in the paper.

TABLE D.7: ACCESSIBILITY AREAS IN THE US

City	$\mathcal{A}^C_{0,15}$	$\mathcal{A}^C_{15,30}$	$\mathcal{A}^C_{30,45}$	$\mathcal{A}^C_{45,60}$	$\mathcal{A}^P_{0,15}$	$\mathcal{A}^P_{15,30}$	$\mathcal{A}^P_{30,45}$	$\mathcal{A}^P_{45,60}$
Albany, NY	51.81	479.2	1115	1883	2.905	30.66	80.31	79.81
Atlanta, GA	123.3	1037	1845	2972	4.484	44.89	159.6	287.9
Austin, TX	75.49	1025	1977	3065	2.669	20.44	61.91	102.1
Birmingham, AL	209.7	1103	2016	3414	2.805	8.265	32.97	42.49
Boston, MA	23.51	424.7	1231	2171	5.634	49.80	103.5	147.6
Buffalo, NY	74.82	490.9	806.3	1322	5.415	30.10	54.23	80.44
Charlotte, NC	63.56	637.4	1403	2093	3.554	30.78	114.9	170.5
Chicago, IL	43.56	616.3	1768	2129	9.311	72.79	204.4	284.0
Cincinnati, OH	32.14	490.6	1339	2025	3.724	25.46	96.88	147.0
Cleveland, OH	61.18	502.1	1219	2031	5.590	38.04	107.6	174.7
Columbus, OH	65.34	791.6	1565	3160	3.970	31.23	72.15	114.9
Dallas, TX	142.4	1799	3489	4735	2.565	26.36	117.6	204.0
Denver, CO	9.095	503.4	1782	2395	3.824	31.98	113.5	197.3
Detroit, MI	68.41	614.8	1370	1878	3.014	28.36	69.59	139.1
Fresno, CA	180.6	797.4	1375	2010	3.389	24.71	60.38	78.69
Hartford, CT	147.1	852.1	1704	2472	5.549	48.12	149.5	204.9
Houston, TX	349.6	1966	3352	4029	2.805	27.64	124.5	283.4
Indianapolis, IN	43.46	626.4	1658	3271	2.574	36.81	96.47	129.3
Jacksonville, FL	52.80	456.8	886.4	1261	2.445	12.79	47.32	81.53
Kansas City, MO	102.4	1045	2157	3213	4.279	31.66	65.31	110.6
Las Vegas, NV	188.1	961.0	686.8	733.3	3.144	19.45	63.16	138.1
Los Angeles, CA	164.4	1369	1864	2199	4.179	45.52	158.0	347.0
Louisville, KY	51.79	660.6	1328	2011	3.082	21.27	71.02	88.31
Memphis, TN	174.3	1041	2287	3606	2.649	23.09	46.00	67.05
Miami, FL	27.64	344.6	750.6	859.4	2.248	25.85	67.45	134.1
Milwaukee, WI	49.52	503.4	1313	2200	3.005	25.08	97.48	138.7
Minneapolis, MN	60.47	1066	1942	3168	3.584	27.13	127.6	255.6
Nashville, TN	145.2	1068	2647	4182	2.344	22.72	83.39	82.53
New Haven, CT	13.20	308.1	767.6	1301	3.509	36.11	72.54	87.45
New Orleans, LA	142.4	403.3	427.8	840.9	3.064	18.81	62.44	85.36
New York, NY	22.36	427.5	1424	2208	5.285	46.33	152.2	323.3
Oklahoma City, OK	99.40	1114	2197	3431	2.085	18.63	84.95	101.0
Orlando, FL	77.48	665.6	1400	1399	2.394	12.47	44.77	102.9
Philadelphia, PA	62.95	590.2	1717	2881	12.12	81.89	196.0	290.1
Phoenix, AZ	30.57	636.7	1888	2196	2.900	29.99	105.1	214.3
Pittsburgh, PA	105.6	613.4	1415	2540	4.505	53.82	143.4	165.8
Portland, OR	19.69	493.5	1286	1911	3.478	33.85	101.6	171.8
Raleigh, NC	21.86	253.6	906.6	1722	3.659	22.99	66.19	97.77
Richmond, VA	58.24	668.9	1267	1894	3.199	24.87	47.27	63.95
Sacramento, CA	93.16	785.3	1841	2993	3.008	18.38	54.63	104.3
Salt Lake City, UT	54.12	659.7	987.5	1523	3.843	25.27	83.58	131.1
San Antonio, TX	231.8	1488	2446	3606	2.864	20.88	93.65	179.7
San Diego, CA	84.54	669.0	777.2	981.4	2.915	16.57	57.99	137.9
San Francisco, CA	32.02	367.0	835.9	1629	8.252	43.50	90.31	142.0
Seattle, WA	50.64	533.3	914.2	1362	4.660	35.34	159.8	249.4
St. Louis, MO	120.6	926.0	1860	2859	3.054	16.65	78.03	156.5
St. Petersburg, FL	71.39	202.4	539.9	1126	5.027	33.50	64.31	57.83
Tampa, FL	61.05	478.8	1014	1468	2.168	10.54	42.69	82.71
Tucson, AZ	81.87	568.6	1182	1574	5.121	24.76	80.23	79.10
Tulsa, OK	87.74	1005	1960	2894	2.245	15.30	61.83	58.02
Virginia Beach, VA	49.45	318.4	557.3	670.0	2.457	8.169	22.84	35.47
Washington, DC	14.88	302.5	1164	2040	3.905	34.59	128.2	367.0
Average	85.94	725.9	1493	2260	3.855	29.70	91.18	149.9

Notes: The table presents the size of the area from which the CBD of a given city is accessible within (0,15)-, (15,30)-, (30,45)-, or (45,60)-minute commutes via either cars or public transit. The areas have been constructed for a Wednesday at 8:45 AM. The areas are computed using TravelTime Technologies's Isochrone API.

TABLE D.8: ACCESSIBILITY ZONE AREAS IN EUROPE

City	$\mathcal{A}^C_{0,15}$	$\mathcal{A}^C_{15,30}$	$\mathcal{A}^C_{30,45}$	$\mathcal{A}^C_{45,60}$	$\mathcal{A}^P_{0,15}$	$\mathcal{A}^P_{15,30}$	$\mathcal{A}^P_{30,45}$	$\mathcal{A}^P_{45,60}$
Amsterdam, Netherlands	54.27	546.2	1563	2558	7.015	56.32	156.8	357.0
Athens, Greece	10.02	144.6	450.6	569.3	10.69	81.38	130.3	133.7
Barcelona, Spain	5.019	27.83	230.6	646.1	9.081	62.66	116.6	207.4
Berlin, Germany	21.29	79.42	253.8	799.8	7.773	89.44	234.6	420.6
Birmingham, UK	57.97	675.9	1791	3047	2.814	29.81	105.7	200.0
Bordeaux, France	7.448	56.31	267.2	549.7	2.938	30.68	86.68	131.9
Bremen, Germany	39.30	435.8	1206	2536	5.040	37.34	105.4	143.7
Brussels, Belgium	15.07	252.7	1527	3476	8.309	98.72	237.2	555.5
Budapest, Hungary	20.74	178.1	708.1	1732	3.806	51.74	143.2	213.6
Cologne, Germany	26.24	395.9	1587	3509	5.550	64.92	206.6	422.2
Copenhagen, Denmark	25.16	140.0	597.3	1264	14.00	88.04	209.1	307.7
Dortmund, Germany	13.79	343.1	1310	2622	7.496	57.19	135.0	251.3
Dresden, Germany	30.55	192.2	793.4	1869	4.831	49.80	109.2	155.4
Dublin, Ireland	26.05	306.5	1194	2047	4.866	40.00	126.8	202.1
Duesseldorf, Germany	33.02	544.0	1930	3607	3.459	42.08	112.6	267.2
Frankfurt, Germany	16.93	264.3	1320	2547	11.05	85.13	245.1	437.3
Glasgow, UK	51.21	608.3	1420	2058	5.445	53.22	173.7	294.7
Hamburg, Germany	17.11	145.6	712.9	1826	7.251	61.10	214.5	379.2
Hanover, Germany	32.18	327.9	1169	2125	10.98	78.24	138.2	215.2
Helsinki, Finland	6.696	75.93	404.9	889.7	9.017	96.46	263.9	232.0
Katowice, Poland	22.90	318.7	984.8	1630	1.425	21.60	107.0	184.2
Krakow, Poland	20.91	143.3	398.3	895.4	6.232	58.74	121.7	167.5
Leeds, UK	44.54	425.7	1223	2275	4.258	33.12	115.4	268.9
Lille, France	6.278	95.58	489.7	1775	2.624	37.68	93.83	130.0
Lisbon, Portugal	18.07	344.3	685.1	1093	3.104	19.60	66.73	131.3
Liverpool, UK	29.37	193.5	567.5	1147	2.844	26.60	122.5	184.5
London, UK	12.00	63.08	173.5	479.9	3.383	39.74	248.9	618.0
Lyon, France	2.759	62.23	300.3	698.4	7.803	62.22	157.9	230.4
Madrid, Spain	5.344	192.9	869.8	1474	14.50	198.0	421.3	426.5
Manchester, UK	33.39	258.4	999.9	1975	3.384	28.07	152.7	313.8
Marseille, France	6.437	74.93	238.1	522.2	4.833	39.88	85.27	67.54
Milan, Italy	3.180	27.02	166.1	917.0	9.370	76.72	140.4	274.1
Munich, Germany	31.46	421.2	1670	3332	6.534	99.11	265.4	378.6
Naples, Italy	21.35	363.4	860.3	873.4	4.825	22.46	53.66	94.90
Nuremberg, Germany	23.21	371.0	1500	3110	4.582	62.41	131.4	198.8
Oslo, Norway	25.94	263.0	697.9	1375	6.769	73.46	176.8	239.7
Paris, France	3.449	23.05	136.2	403.2	13.56	118.2	377.1	712.8
Porto, Portugal	25.31	435.8	1019	1556	6.686	46.71	79.32	90.45
Prague, Czech Republic	21.14	270.6	1099	2633	9.228	110.8	284.5	369.2
Rome, Italy	11.85	85.75	384.9	929.8	9.585	59.34	115.6	138.4
Rotterdam, Netherlands	61.40	656.9	1488	2720	8.315	62.11	176.5	349.6
Seville, Spain	9.687	92.66	432.9	869.7	2.334	10.38	35.19	74.70
Sheffield, UK	14.13	177.6	881.7	1776	4.806	35.90	83.41	127.8
Stockholm, Sweden	29.74	413.6	877.8	1453	2.709	35.51	171.0	337.1
Stuttgart, Germany	30.03	404.9	1337	2074	8.334	74.82	206.4	336.0
Toulouse, France	7.463	72.19	308.5	928.9	9.514	71.89	148.0	167.8
Turin, Italy	13.22	78.60	410.0	993.5	4.254	30.29	68.50	134.7
Valencia, Spain	6.139	92.62	494.0	1206	8.223	48.71	96.75	100.1
Vienna, Austria	6.419	134.3	729.7	1660	6.819	81.78	166.2	208.7
Warsaw, Poland	17.28	121.2	604.4	1287	8.567	94.74	200.3	307.4
Zuerich, Switzerland	33.19	639.7	1563	2492	8.555	84.70	241.5	471.2
Average	21.72	256.1	863.2	1703	6.654	61.17	160.0	262.0

Notes: The table presents the size of the area from which the CBD of a given city is accessible within (0,15)-, (15,30)-, (30,45)-, or (45,60)-minute commutes via either cars or public transit. The areas have been constructed for a Wednesday at 8:45 AM. The areas are computed using TravelTime Technologies's Isochrone API.